

**Impact of linker between triazolyl-uracil and phenanthridine on recognition of DNA and RNA.
Recognition of uracil – containing RNA.**

Dijana Saftić^a, Marijana Radić Stojković^a, Biserka Žinić^a, Ljubica Glavaš-Obrovac^b, Marijana Jukić^b, Ivo Piantanida^a, Lidija-Marija Tumir^{a*}

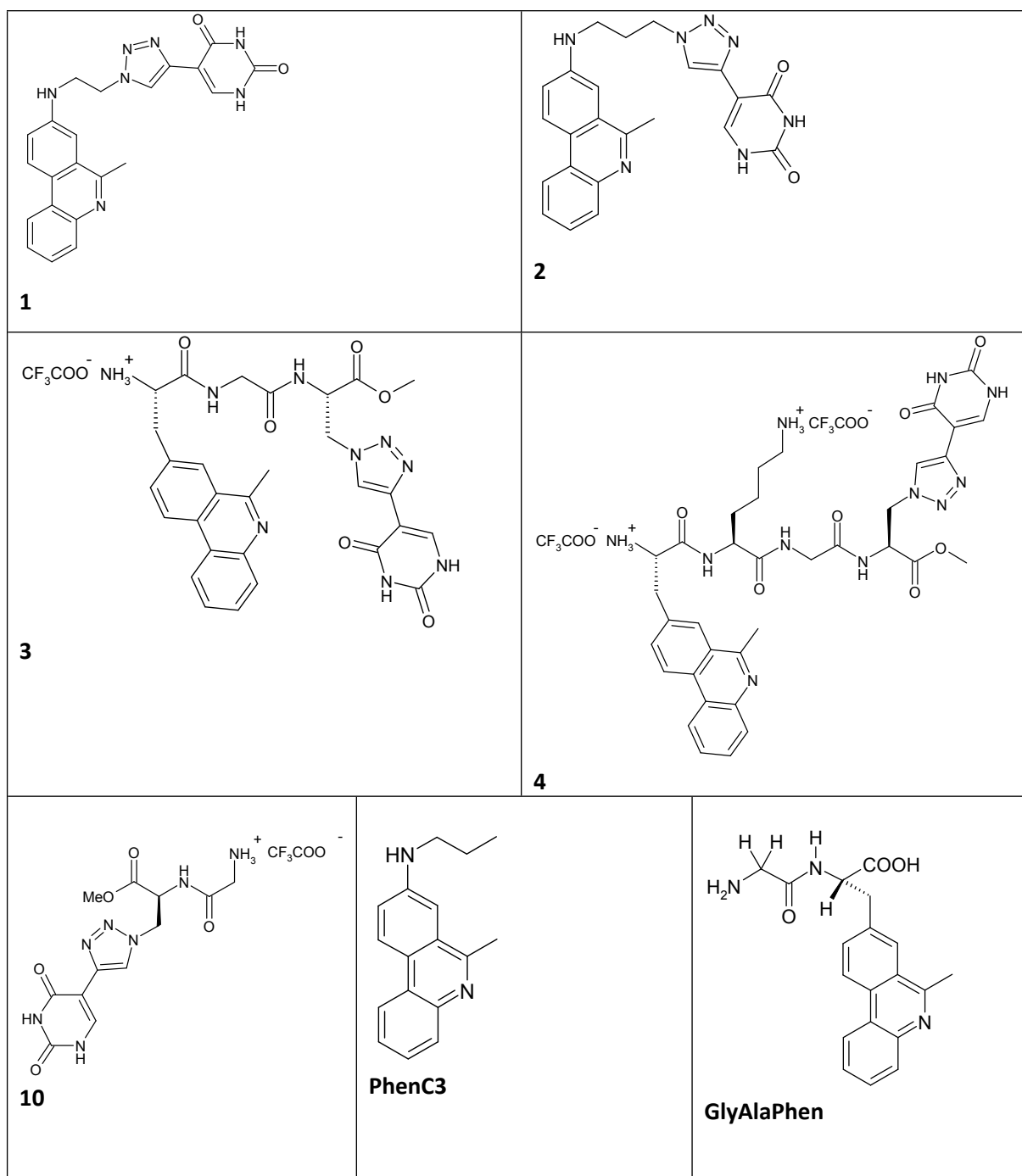
^aLaboratory for Biomolecular Interactions and Spectroscopy, Division of Organic Chemistry & Biochemistry, Ruđer Bošković Institute, HR 10002 Zagreb, P.O.B. 180, Croatia. Fax: +385 1 46 80 195; Tel: +385 1 45 71 210; E-mail: tumir@irb.hr

^bDepartment of Medicinal Chemistry and Biochemistry, School of Medicine Osijek, 31000 Osijek, Croatia

SUPPORTING INFORMATION

Content

1. General Procedures
2. Spectroscopic properties of **1-4**
3. Interactions of **1-4** with DNA/RNA
4. Biology
5. MM2 calculations



Scheme S1. Structures of examined compounds 1-4, referent compound DS8 and previously published referent compounds PhenC3¹ and GlyAlaPhen².

1. General procedures

Solvents were distilled from appropriate drying agents shortly before use. TLC was carried out on DC-plastikfolien Kieselgel 60 F₂₅₄ and preparative thick layer (2 mm) chromatography was done on Merck 60 F₂₅₄. Microwave assisted reaction was conducted in a borosilicate glass vials sealed by reusable snap-cap with PTFE coated silicone septum. The microwave heating was performed in the Anton Paar microwave synthesis reactor Monowave 300. Reaction mixtures were stirred with a magnetic stir bar during the irradiation. The temperature, pressure and irradiation power were monitored during the course of the reaction. After completed irradiation, the reaction tube was cooled with high-pressure air until the temperature had fallen below 55 °C (ca. 1 min). IR spectra were obtained as KBr pellets on a Perkin–Elmer 297 spectrophotometer. ¹H and ¹³C NMR spectra were recorded in DMSO-*d*₆ or CDCl₃ on Bruker AV 300 and 600 MHz spectrometers using TMS as the internal standard. The assignation of C-atoms and protons were confirmed on the basis of 2D NMR HETCOR, COSY, and NOESY. Chemical shifts (δ) are expressed in ppm, and *J* values in Hz. Signal multiplicities are denoted as s (singlet), d (doublet), t (triplet), q (quartet) and m (multiplet). High resolution mass spectra (HRMS) were obtained using a MALDI-TOF/TOF mass spectrometer 4800 Plus MALDI TOF/TOF analyzer (Applied Biosystems Inc., Foster City, CA, USA). The electronic absorption spectra of newly prepared compounds, UV-Vis titration and thermal melting experiments were measured on a Varian Cary 100 Bio spectrometer. Fluorescence spectra were recorded on Varian Cary Eclipse fluorimeter. CD spectra were recorded on JASCO J815 spectrophotometer. UV-Vis, fluorescence and CD spectra were recorded using appropriate 1 cm path quartz cuvettes.

Materials

Starting compounds were prepared according to published procedures³⁻⁴. Polynucleotides were purchased as noted: *calf thymus* (ct)-DNA, poly dGdC – poly dGdC, poly dAdT – poly dAdT, poly rA – poly rU, poly rA and poly rU (Sigma) and dissolved in sodium cacodylate buffer, *I* = 0.05 mol dm⁻³, pH=7.0. The *calf thymus* (ct-) DNA was additionally sonicated and filtered through a 0.45 μm filter⁵. Polynucleotide concentration was determined spectroscopically as the concentration of phosphates⁶. It is important to note that at experimental conditions (pH = 5) poly rA was protonated and formed double helix⁷. The double-stranded conformation of poly rAH⁺-poly rAH⁺ was obtained by lowering the pH value from the initial value of 7.0 to 5.0 and its concentration directly derived from the concentration of single stranded poly rA. The formation of ds-poly rAH⁺-poly rAH⁺ was confirmed by CD and thermal melting experiments.^{8,9}

UV/Vis, fluorescence and CD measurements

The measurements were performed by adding aliquots of DMSO stock solutions to the buffer solution (pH = 5, *I* = 0.05 mol dm⁻³, sodium cacodylate/HCl buffer, DMSO content of the final solutions <0.01%). Concentrations below 4 × 10⁻⁵ M were used for UV-Vis absorbance measurement to avoid intermolecular association. Under the experimental conditions used (concentration of compounds **1-4** ~ 2 × 10⁻⁵ mol dm⁻³ for UV-Vis and ~ 2 × 10⁻⁶ mol dm⁻³ for fluorescence) the absorbance and fluorescence intensities of **1-4** were proportional to their concentrations.

Fluorimetric titrations were performed by adding portions of polynucleotide solution into the solution of the studied compound. Excitation wavelength of λ_{exc} ≥ 300 nm was used to avoid

absorption of excitation light caused by increasing absorbance of the polynucleotide. After mixing polynucleotides with studied compounds it was observed in all cases that equilibrium was reached in less than 120 seconds. In following 2-3 hours fluorescence spectra of complexes remained constant. Due to low concentrations of studied compounds and polynucleotides used in fluorimetric titrations no precipitation occurred¹⁰. Emission was collected in the range $\lambda_{em}=470 - 700$ nm (for compounds **1** and **2**) and $\lambda_{em}=330 - 550$ nm (for compounds **3** and **4**). Fluorescence spectra were collected at $r < 0.3$ ($r = [\text{compound}] / [\text{polynucleotide}]$) to assure one dominant binding mode. Titration data obtained for ds-DNA and ds-RNA were processed by means of Scatchard equation¹¹ and Global Fit procedure¹². Calculations gave values of ratio $n=0.1\pm 0.05$, but for easier comparison all K_s values were re-calculated for fixed $n=0.1$. Values for K_s have satisfactory correlation coefficients (>0.98). In Scatchard equation values of stability constant (K_s) and ratio ($n=[\text{bound compound}] / [\text{polynucleotide}]$) are highly mutually dependent and similar quality of fitting calculated to experimental data is obtained for $\pm 20\%$ variation for K_s and n ; this variation can be considered as an estimation of the errors for the given binding constants.

CD experiments were performed by adding portions of compound stock solution into the solution of polynucleotide ($c \approx 2 \times 10^{-5}$ mol dm⁻³). CD spectra with scanning speed of 200 nm/min. Buffer background was subtracted from each spectra, while each spectra was result of five accumulations. Examined compounds **1-2** are achiral and therefore do not possess intrinsic CD spectrum. Compounds **3** and **4** were built by chiral amino acid building blocks and consequently have intrinsic CD spectrum of low intensity.

Thermal melting curves for ds-DNA, ds-RNA and their complexes with studied compounds were determined by following the absorption change at 260 nm a function of temperature¹³. Absorbance scale was normalized. T_m values are the midpoints of the transition curves determined from the maximum of the first derivative and checked graphically by the tangent method. The ΔT_m values were calculated subtracting T_m of the free nucleic acid from T_m of the complex. Every ΔT_m value here reported was the average of at least two measurements. The error in ΔT_m is ± 0.5 °C.

Cytotoxicity evaluation^{14,15}

Cytotoxic effects on the normal and tumours cells' growth were determined using the colorimetric methyltetrazolium (MTT) assay. Experiments were carried out on two tumour human cell lines (HeLa and CaCo-2) and on one canine cell line (MDCK I) as normal cells. The adherent cells, MDCK1, HeLa, and CaCO2, were seeded in 96 micro-well plates at a concentration of 2×10^4 cells per mL and allowed to attach overnight in a CO2 incubator (IGO 150 CELLlife™, JOUAN, Thermo Fisher Scientific, Waltham, MA, USA). After 72 hours of exposure to tested compounds, the medium was replaced with 5 mg mL⁻¹ MTT solution and the resulting formazan crystals were dissolved in DMSO. To each well, 10% SDS with 0.01 mol L⁻¹ HCl was added to dissolve water-insoluble MTT-formazan crystals overnight. An Elisa microplate reader (iMark, BIO RAD, Hercules, CA, USA) was used for measurement of absorbance at 595 nm. All experiments were performed at least three times in triplicate. The percentage of cell growth (PG) was calculated using the following equation:

$$PG = (A_{\text{compound}} - A_{\text{background}}) / (A_{\text{control}} - A_{\text{background}}) \times 100$$

where $A_{\text{background}}$ at the adherent cells is the absorbance of MTT solution and DMSO; $A_{\text{background}}$ at the suspension cells is the absorbance of the medium without cells, but containing MTT and 10% SDS

with 0.01 mol L⁻¹ HCl; and A_{control} is the absorbance of the cell suspension grown without tested compounds.

2. Spectroscopic properties of **1-4**

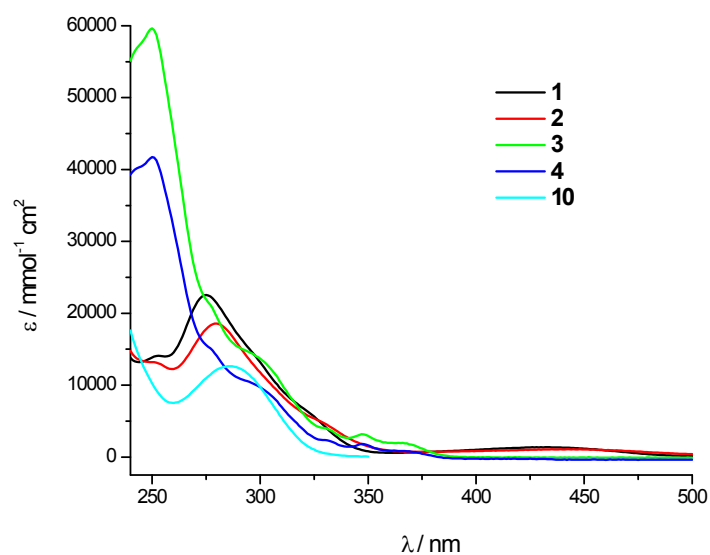


Figure S1. UV-Vis spectra of **1-4** and reference **10**, $c=1 - 4 \times 10^{-5}$ M, pH = 5.0, Na-cacodylate buffer, $I=0.05$ M.

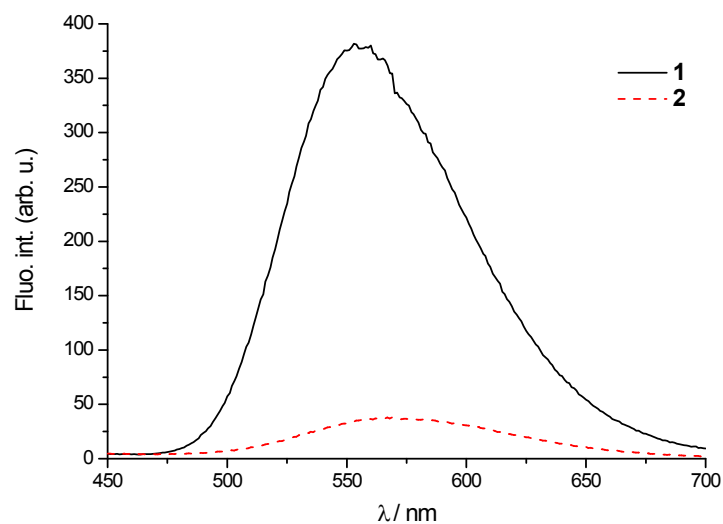


Figure S2. Fluorescence spectra of **1** and **2**, $c=2 \times 10^{-6}$ M, $\lambda_{\text{exc}} = 280$ nm, slit exc = 5 nm, slit em = 5 nm, pH = 5.0, Na-cacodylate buffer, $I=0.05$ M.

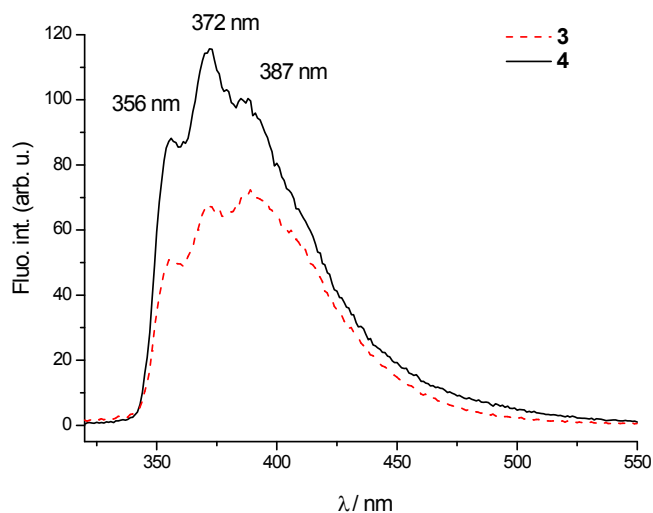


Figure S3. Fluorescence spectra of **3** and **4**, $c=2 \times 10^{-6}$ M, $\lambda_{\text{exc}} = 250$ nm, slit exc = 5 nm, slit em = 5 nm pH = 5.0, Na-cacodylate buffer, $I=0.05$ M.

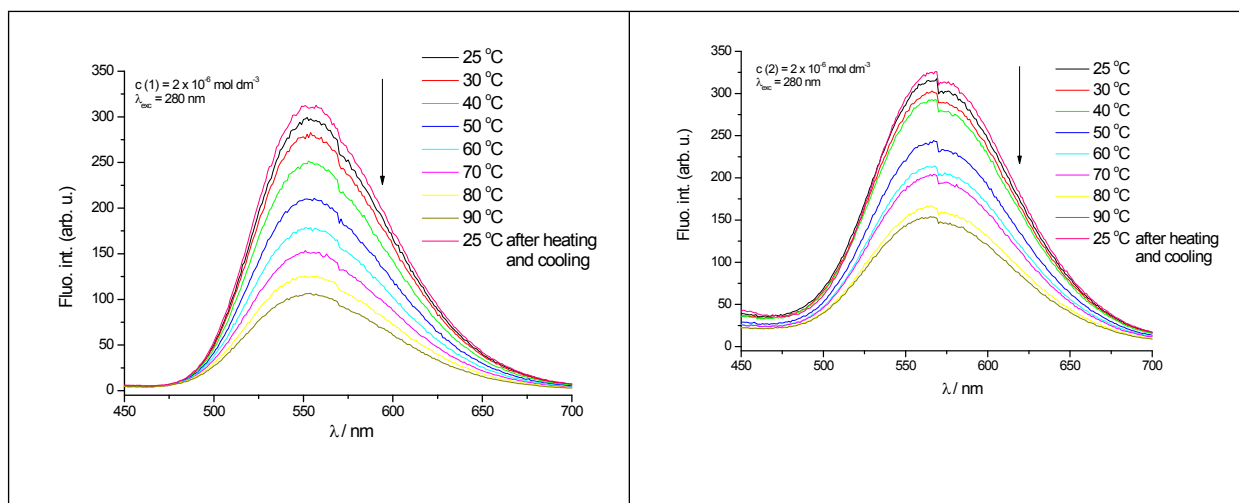


Figure S4. Influence of temperature increase ($T = 25^\circ\text{C} - 90^\circ\text{C}$) on fluorescence emission spectra of **1** (left) and **2** (right), $c=2 \times 10^{-6}$ M, $\lambda_{\text{exc}} = 280$ nm, pH = 5.0, Na-cacodylate buffer, $I=0.05$ M.

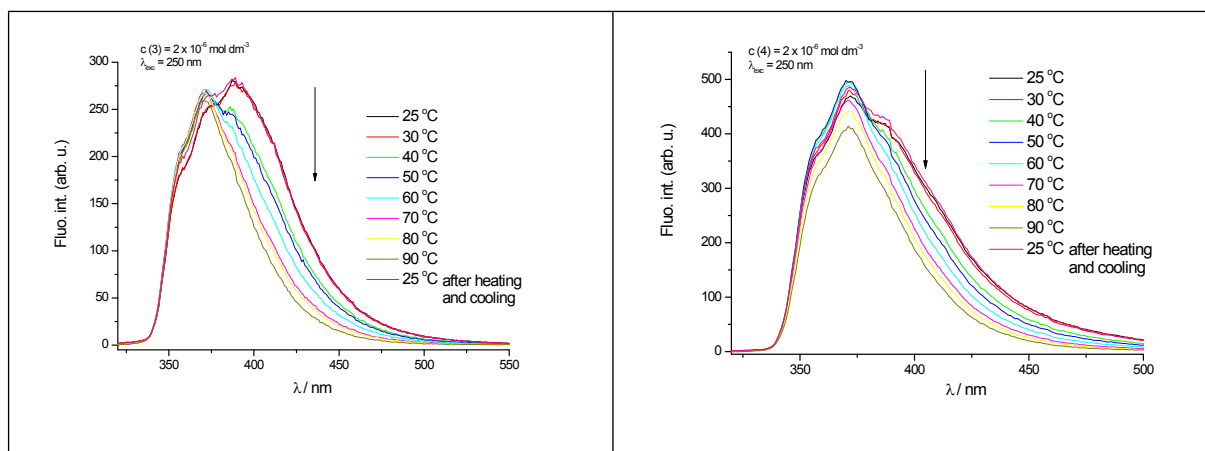


Figure S5. Influence of temperature increase ($T = 25^\circ\text{C} - 90^\circ\text{C}$) on fluorescence emission spectra of **3** (left) and **4** (right), $c=2 \times 10^{-6}$ M, $\lambda_{\text{exc}} = 250$ nm, pH = 5.0, Na-cacodylate buffer, $I=0.05$ M.

3. Interactions of 1-4 with DNA/RNA

Table S1. Groove widths and depths for selected nucleic acid conformations.^{10,16}

	Groove width [Å]		Groove depth [Å]	
	major	minor	major	minor
^a poly dAdT – poly dAdT	11.2	6.3	8.5	7.5
^b poly dA – poly dT	11.4	3.3	7.5	7.9
^c poly rA- poly rU	3.8	10.9	13.5	2.8
^a poly dGdC – poly dGdC	13.5	9.5	10.0	7.2

^a B-helical structure (e.g. B-DNA); ^b C-helical structure (e.g. C-DNA). ^c A-helical structure (e.g. A-DNA).

3.1. Thermal melting experiments

Table S2. The ^a ΔT_m values (°C) of studied ds-polynucleotides upon addition of **1-4** (ratio $r^b = 0.3$ or $r^d = 0.1$) at pH = 5.0 (buffer sodium cacodylate, $I = 0.05 \text{ mol dm}^{-3}$), $c(\text{DNA} / \text{RNA}) = 1\text{-}2 \times 10^{-5} \text{ M}$.

Compound	$\Delta T_m / ^\circ\text{C}$		
	ct-DNA	poly dAdT – poly dAdT	poly rA – poly rU
1	0.9	1.2	-0.6/0 ^c
2	1.0	0.5	-1.0/-0.9 ^c
3	0	1.4	-1.3/-0.7 ^c
4	1.5	2.7	0.8/0 ^d

^a Error in $\Delta T_m : \pm 0.5^\circ\text{C}$;

^b $r = [\text{compound}] / [\text{polynucleotide}]$;

^c biphasic transitions: the first transition at $T_m = 47^\circ\text{C}$ is attributed to denaturation of poly rA-poly rU and the second transition at $T_m = 69^\circ\text{C}$ is attributed to denaturation of poly rAH⁺-poly rAH⁺ since poly rA at pH=5 is mostly protonated and forms ds-polynucleotide. ⁴

^d $r = 0.1$

^e not determined

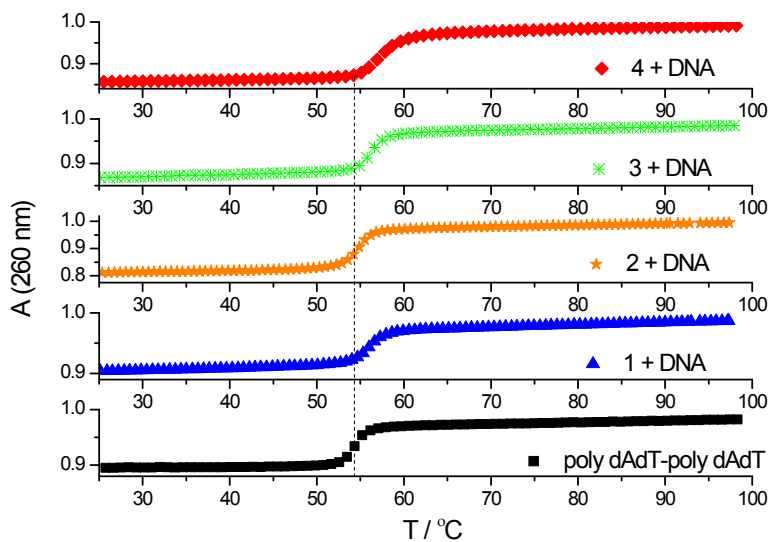


Figure S 6. Melting curves of poly dAdT – poly dAdT upon addition of **1-4** ($c(\text{DNA}) = 1.5\text{-}2 \times 10^{-5} \text{ M}$; ratio $r[\text{compound}] / [\text{polynucleotide}] = 0.3$) at pH = 5.0 (sodium cacodylate buffer, $I = 0.05 \text{ mol dm}^{-3}$)

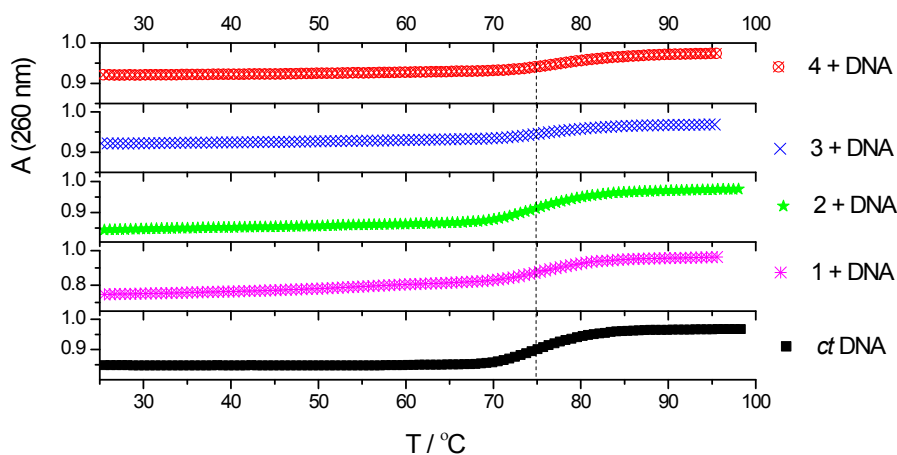


Figure S 7. Melting curves of *ct*-DNA upon addition of **1-4** ($c(\text{DNA}) = 1\text{-}2 \times 10^{-5} \text{ M}$; ratio $r[\text{compound}] / [\text{polynucleotide}] = 0.3$) at pH = 5.0 (sodium cacodylate buffer, $I = 0.05 \text{ mol dm}^{-3}$).

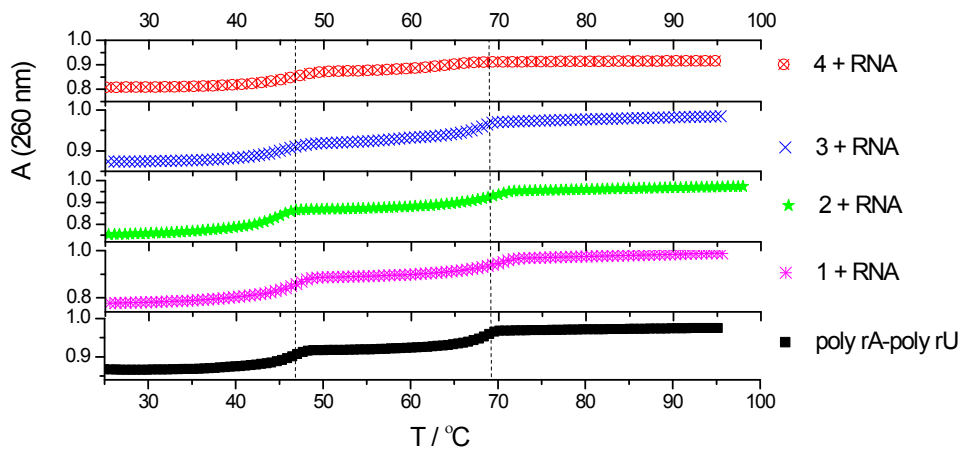


Figure S 8. Melting curves of poly rA-poly rU upon addition of **1-4** ($c(\text{RNA}) = 1\text{-}3 \times 10^{-5} \text{ M}$; ratio $r[\text{compound}] / [\text{polynucleotide}] = 0.1\text{-}0.3$) at $\text{pH} = 5.0$ (sodium cacodylate buffer, $I = 0.05 \text{ mol dm}^{-3}$).

3.2. Fluorimetric titrations

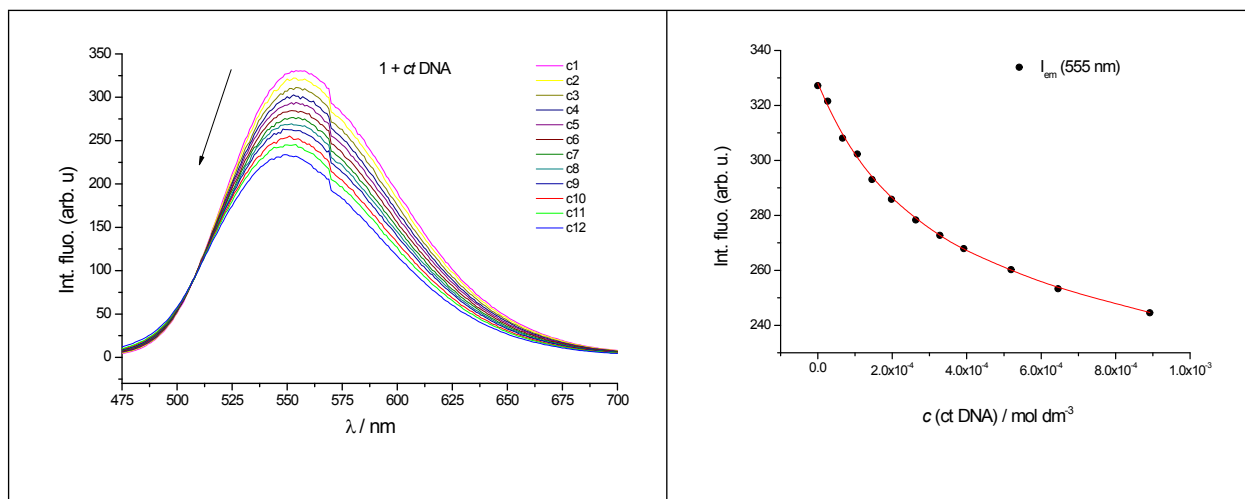


Figure S 9. Left: Fluorimetric titration of **1**, $\lambda_{\text{exc}} = 440 \text{ nm}$, $c = 2 \times 10^{-6} \text{ mol dm}^{-3}$ with ct DNA, Right: Experimental (\bullet) and calculated ($-$) (by Scatchard eq., Table S2) fluorescence intensities of **1** at $\lambda_{\text{em}} = 555 \text{ nm}$ upon addition of ct DNA ($\text{pH} = 5.0$, Na cacodylate buffer, $I = 0.05 \text{ mol dm}^{-3}$).

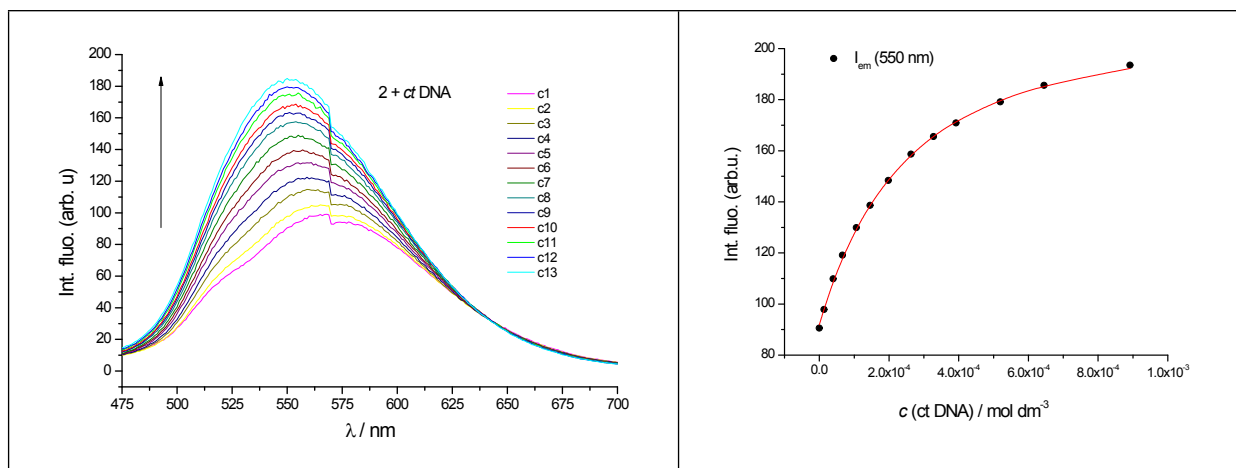


Figure S 10. Left: Fluorimetric titration of **2**, $\lambda_{exc} = 440$ nm, $c = 2 \times 10^{-6}$ mol dm⁻³ with ct DNA, Right: Experimental (●) and calculated (–) (by Scatchard eq., Table S2) fluorescence intensities of **2** at $\lambda_{em} = 550$ nm upon addition of ct DNA (pH = 5.0, Na cacodylate buffer, $I = 0.05$ mol dm⁻³).

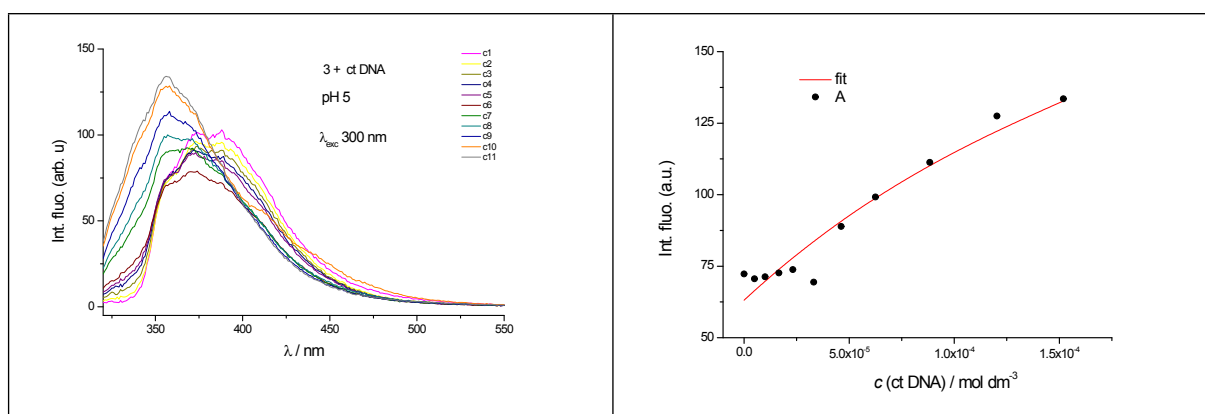


Figure S 11. Left: Fluorimetric titration of **3**, $\lambda_{exc} = 300$ nm, $c = 2 \times 10^{-6}$ mol dm⁻³ with ct DNA, Right: Experimental (●) and calculated (–) (by Scatchard eq., Table S2) fluorescence intensities of **3** at $\lambda_{em} = 357$ nm upon addition of ct DNA (pH = 5.0, Na cacodylate buffer, $I = 0.05$ mol dm⁻³).

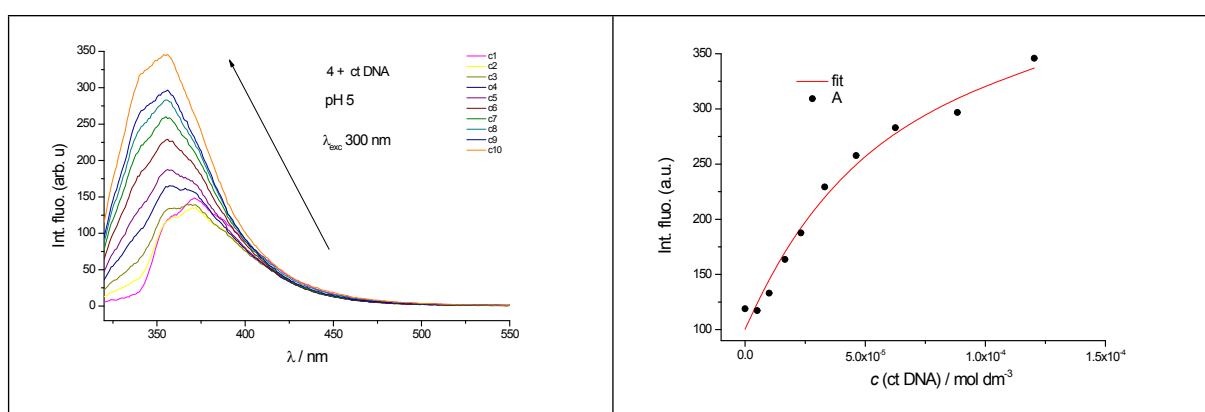


Figure S 12. Left: Fluorimetric titration of **4**, $\lambda_{exc} = 440$ nm, $c = 2 \times 10^{-6}$ mol dm⁻³ with ct DNA, Right: Experimental (●) and calculated (–) (by Scatchard eq., Table S2) fluorescence intensities of **4** at $\lambda_{em} = 357$ nm upon addition of ct DNA (pH = 5.0, Na cacodylate buffer, $I = 0.05$ mol dm⁻³).

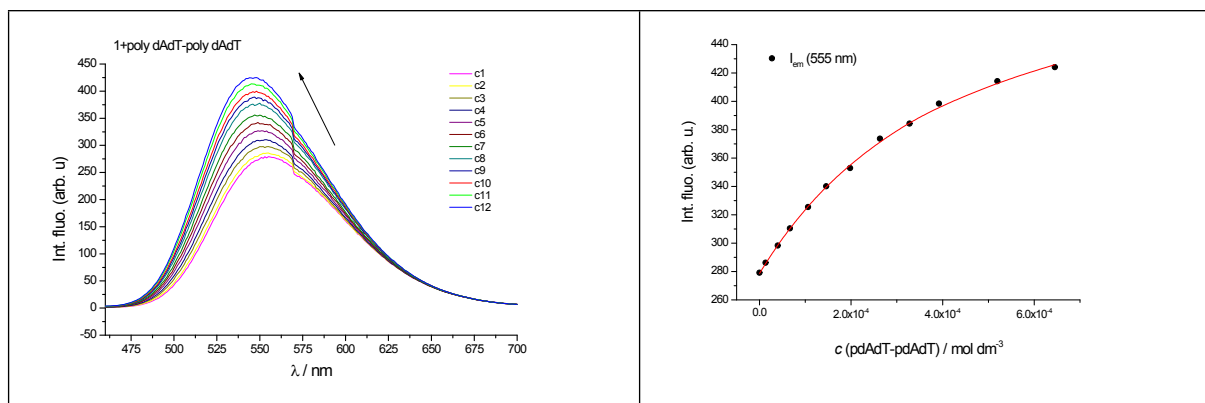


Figure S 13. Left: Fluorimetric titration of **1**, $\lambda_{\text{exc}} = 440 \text{ nm}$, $c = 2 \times 10^{-6} \text{ mol dm}^{-3}$ with poly dAdT-poly dAdT, Right: Experimental (●) and calculated (–) (by Scatchard eq., Table S2) fluorescence intensities of **1** at $\lambda_{\text{em}} = 555 \text{ nm}$ upon addition of ct DNA ($\text{pH} = 5.0$, Na cacodylate buffer, $l = 0.05 \text{ mol dm}^{-3}$).

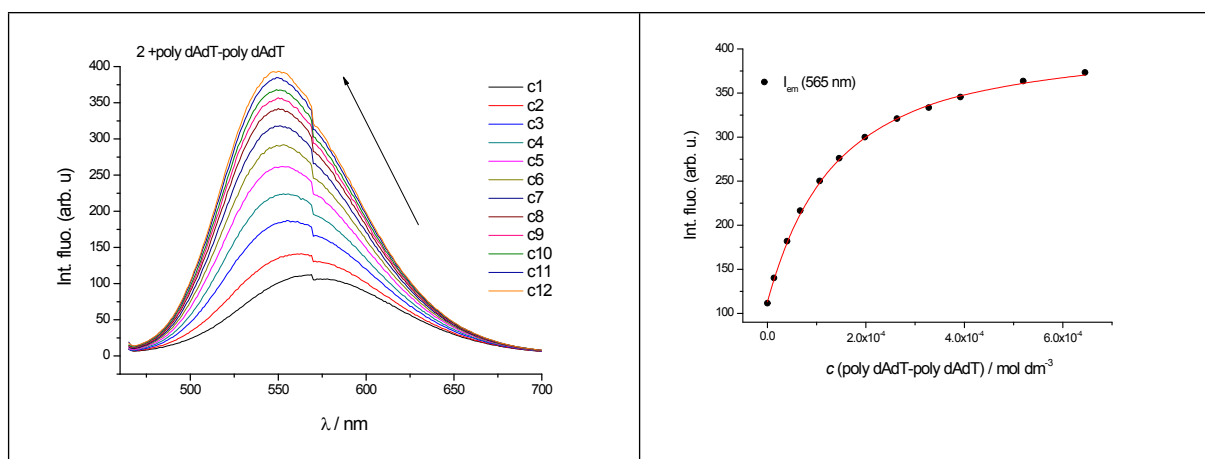


Figure S 14. Left: Fluorimetric titration of **2**, $\lambda_{\text{exc}} = 440 \text{ nm}$, $c = 2 \times 10^{-6} \text{ mol dm}^{-3}$ with poly dAdT-poly dAdT, Right: Experimental (●) and calculated (–) (by Scatchard eq., Table S2) fluorescence intensities of **2** at $\lambda_{\text{em}} = 550 \text{ nm}$ upon addition of ct DNA ($\text{pH} = 5.0$, Na cacodylate buffer, $l = 0.05 \text{ mol dm}^{-3}$).

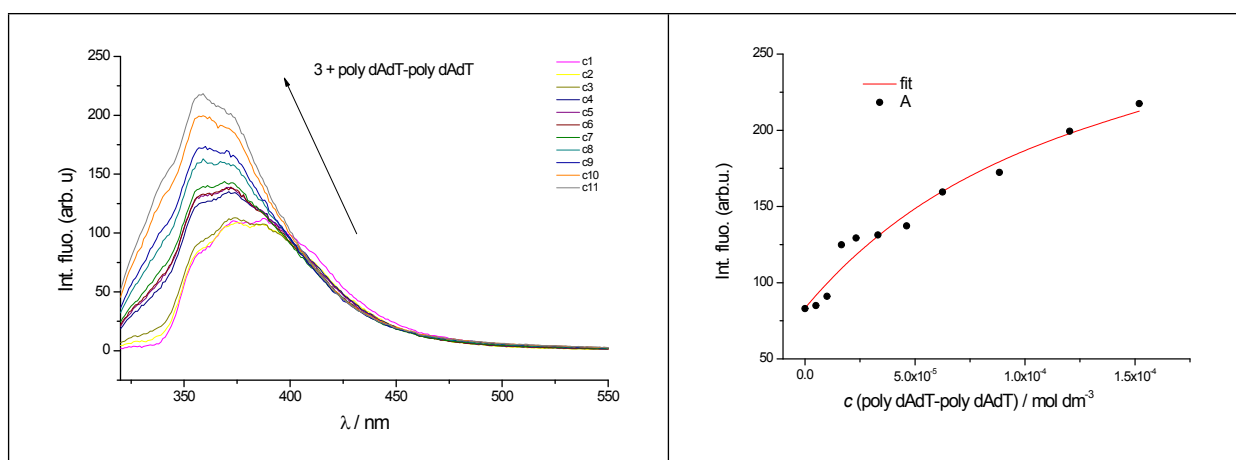


Figure S 15. Left: Fluorimetric titration of **3**, $\lambda_{\text{exc}} = 300 \text{ nm}$, $c = 2 \times 10^{-6} \text{ mol dm}^{-3}$ with poly dAdT-poly dAdT, Right: Experimental (●) and calculated (–) (by Scatchard eq., Table S2) fluorescence intensities of **3** at $\lambda_{\text{em}} = 357 \text{ nm}$ upon addition of ct DNA ($\text{pH} = 5.0$, Na cacodylate buffer, $l = 0.05 \text{ mol dm}^{-3}$).

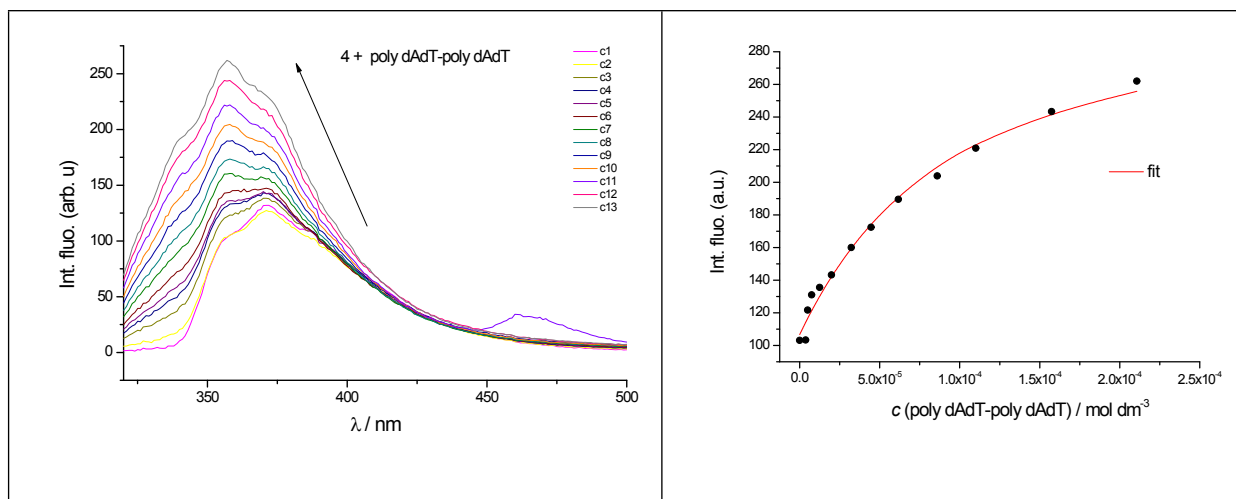


Figure S 16. Left: Fluorimetric titration of **4**, $\lambda_{\text{exc}} = 300 \text{ nm}$, $c = 2 \times 10^{-6} \text{ mol dm}^{-3}$ with poly dAdT-poly dAdT, Right: Experimental (●) and calculated (—) (by Scatchard eq., Table S2) fluorescence intensities of **4** at $\lambda_{\text{em}} = 357 \text{ nm}$ upon addition of ct DNA ($\text{pH} = 5.0$, Na cacodylate buffer, $I = 0.05 \text{ mol dm}^{-3}$).

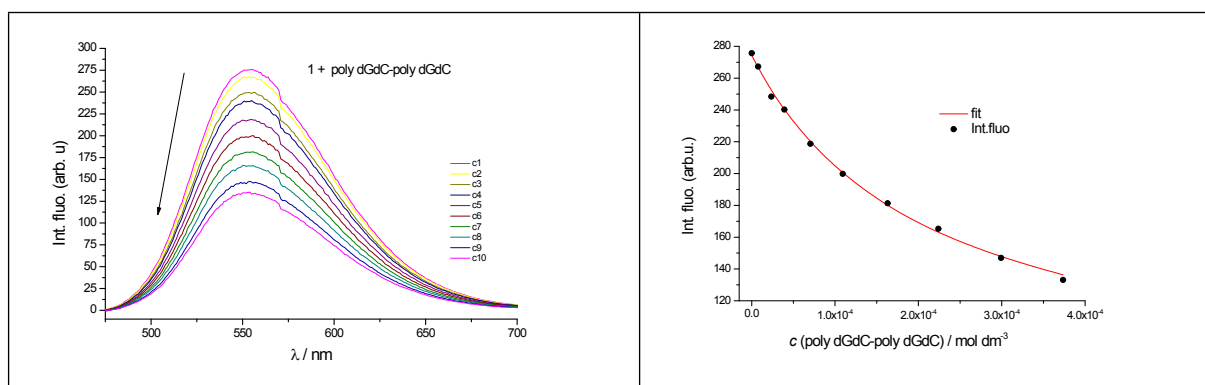


Figure S 17. Left: Fluorimetric titration of **1**, $\lambda_{\text{exc}} = 440 \text{ nm}$, $c = 2 \times 10^{-6} \text{ mol dm}^{-3}$ with poly dGdC-poly dGdC, Right: Experimental (●) and calculated (—) (by Scatchard eq., Table S2) fluorescence intensities of **1** at $\lambda_{\text{em}} = 555 \text{ nm}$ upon addition of ct DNA ($\text{pH} = 5.0$, Na cacodylate buffer, $I = 0.05 \text{ mol dm}^{-3}$).

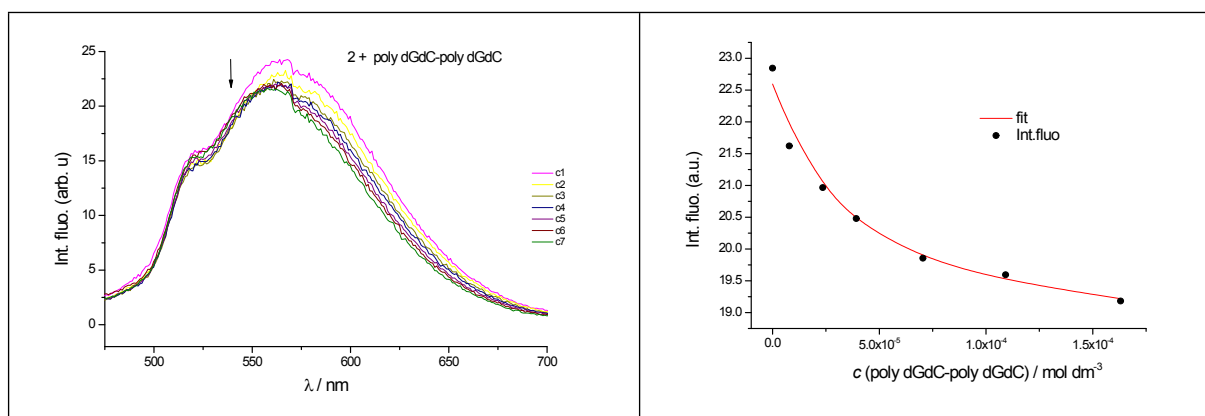


Figure S 18. Left: Fluorimetric titration of **2**, $\lambda_{\text{exc}} = 440 \text{ nm}$, $c = 2 \times 10^{-6} \text{ mol dm}^{-3}$ with poly dGdC-poly dGdC, Right: Experimental (●) and calculated (—) (by Scatchard eq., Table S2) fluorescence intensities of **2** at $\lambda_{\text{em}} = 550 \text{ nm}$ upon addition of ct DNA ($\text{pH} = 5.0$, Na cacodylate buffer, $I = 0.05 \text{ mol dm}^{-3}$).

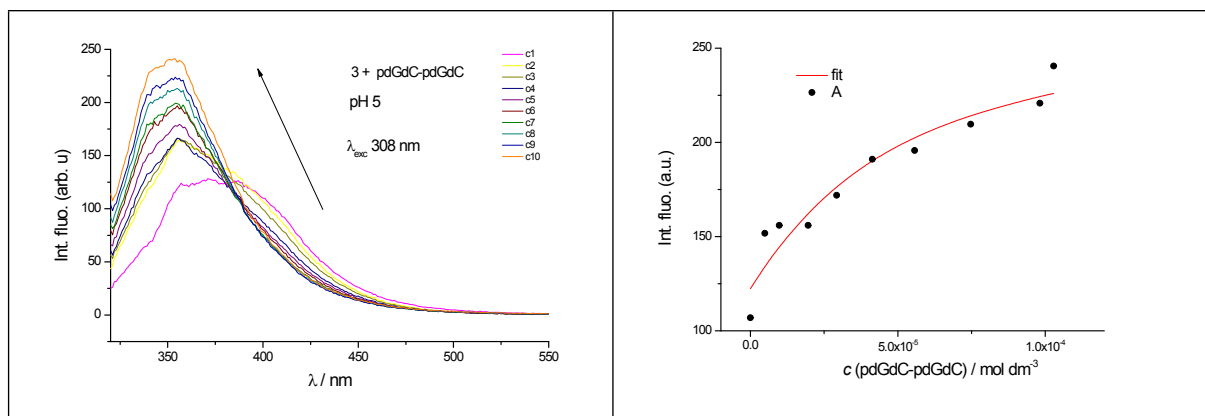


Figure S 19. Left: Fluorimetric titration of **3**, $\lambda_{exc} = 308$ nm, $c = 2 \times 10^{-6}$ mol dm⁻³ with poly dGdC-poly dGdC, Right: Experimental (●) and calculated (–) (by Scatchard eq., Table S2) fluorescence intensities of **3** at $\lambda_{em} = 351$ nm upon addition of ct DNA (pH = 5.0, Na cacodylate buffer, $I = 0.05$ mol dm⁻³).

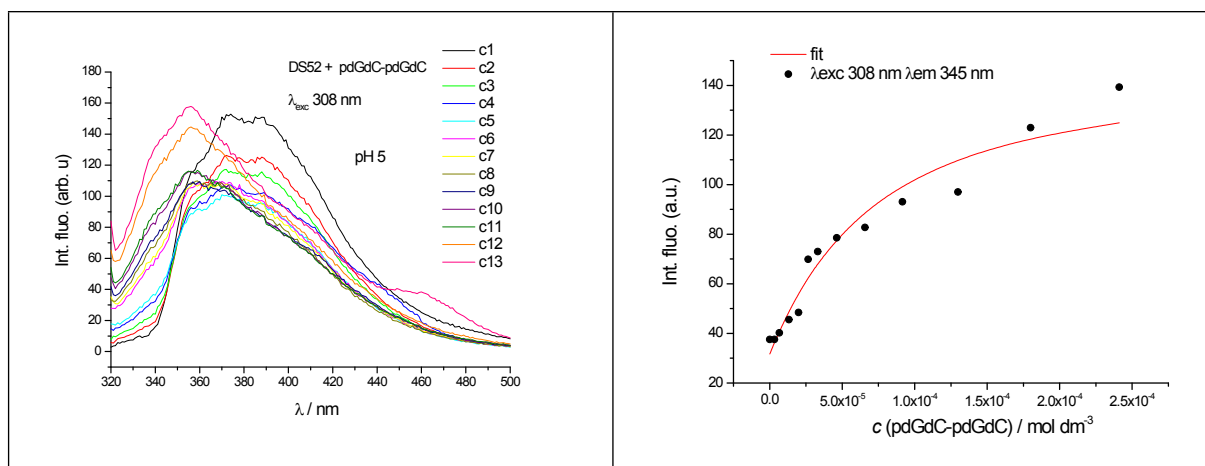


Figure S 20. Left: Fluorimetric titration of **4**, $\lambda_{exc} = 308$ nm, $c = 2 \times 10^{-6}$ mol dm⁻³ with poly dGdC-poly dGdC, Right: Experimental (●) and calculated (–) (by Scatchard eq., Table S2) fluorescence intensities of **4** at $\lambda_{em} = 345$ nm upon addition of ct DNA (pH = 5.0, Na cacodylate buffer, $I = 0.05$ mol dm⁻³).

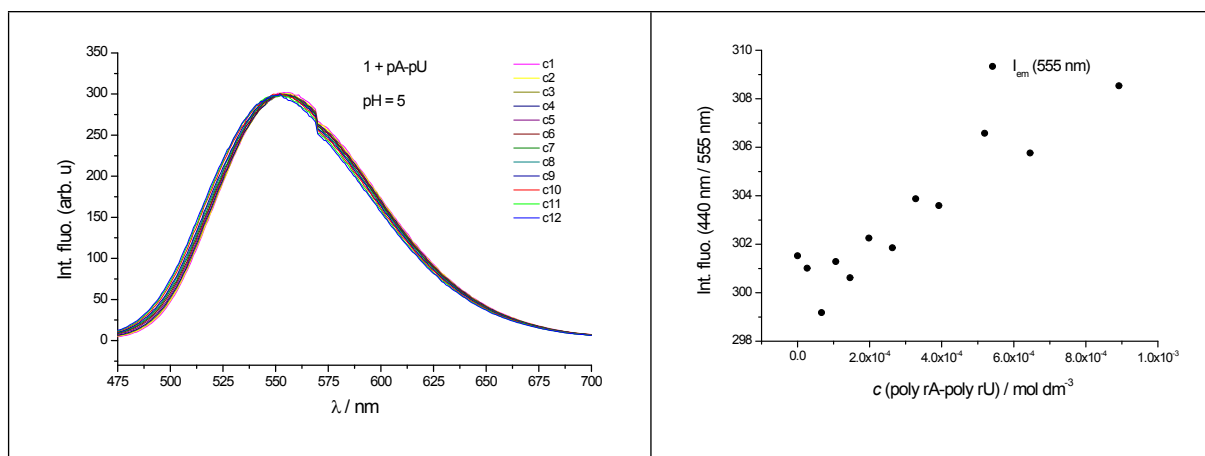


Figure S 21. Left: Fluorimetric titration of **1**, $\lambda_{exc} = 440$ nm, $c = 2 \times 10^{-6}$ mol dm⁻³ with poly rA-poly rU, Right: Experimental (●) fluorescence intensities of **1** at $\lambda_{em} = 555$ nm upon addition of ct DNA (pH = 5.0, Na cacodylate buffer, $I = 0.05$ mol dm⁻³).

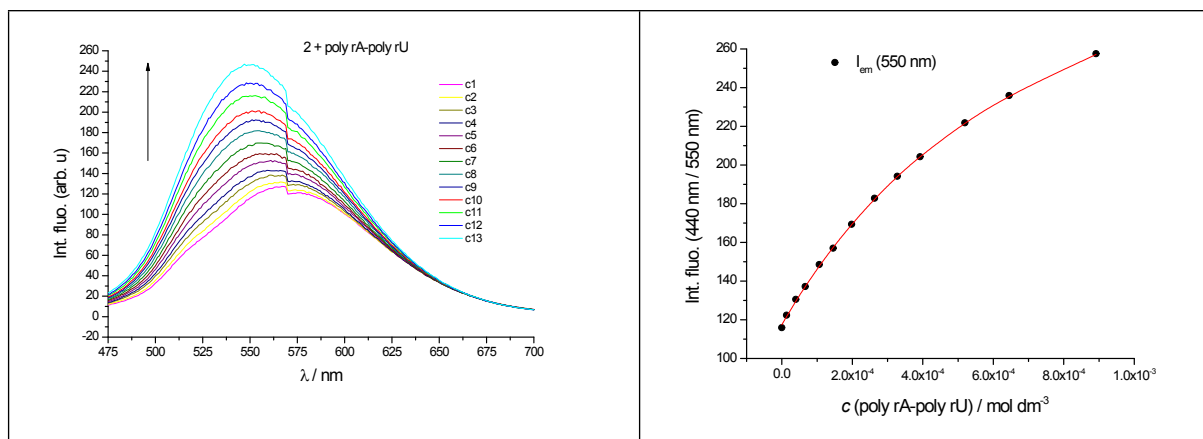


Figure S 22. Left: Fluorimetric titration of **2**, $\lambda_{\text{exc}} = 440 \text{ nm}$, $c = 2 \times 10^{-6} \text{ mol dm}^{-3}$ with poly rA–poly rU, Right: Experimental (●) and calculated (–) (by Scatchard eq., Table S2) fluorescence intensities of **2** at $\lambda_{\text{em}} = 550 \text{ nm}$ upon addition of ct DNA (pH = 5.0, Na cacodylate buffer, $I = 0.05 \text{ mol dm}^{-3}$).

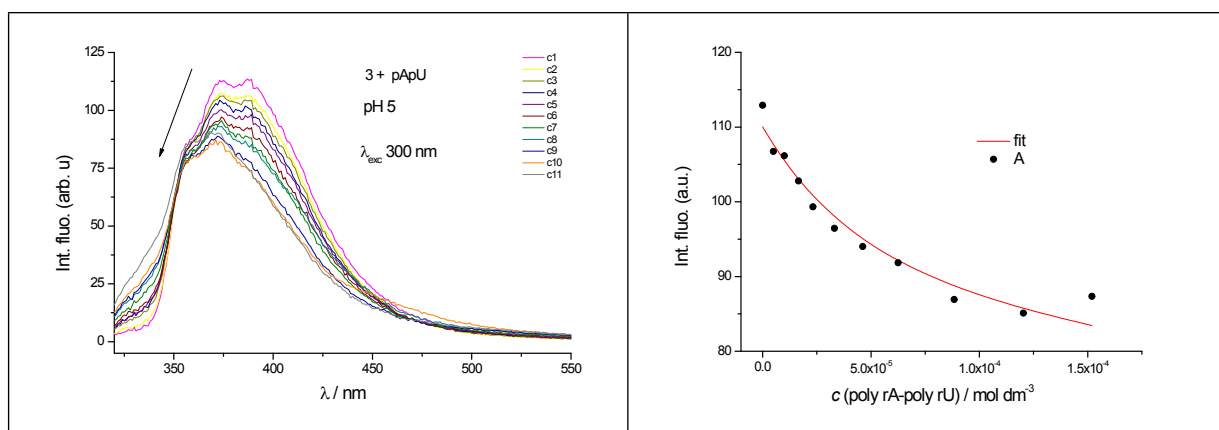


Figure S 23. Left: Fluorimetric titration of **3**, $\lambda_{\text{exc}} = 300 \text{ nm}$, $c = 2 \times 10^{-6} \text{ mol dm}^{-3}$ with poly rA–poly rU, Right: Experimental (●) and calculated (–) (by Scatchard eq., Table S2) fluorescence intensities of **3** at $\lambda_{\text{em}} = 357 \text{ nm}$ upon addition of ct DNA (pH = 5.0, Na cacodylate buffer, $I = 0.05 \text{ mol dm}^{-3}$).

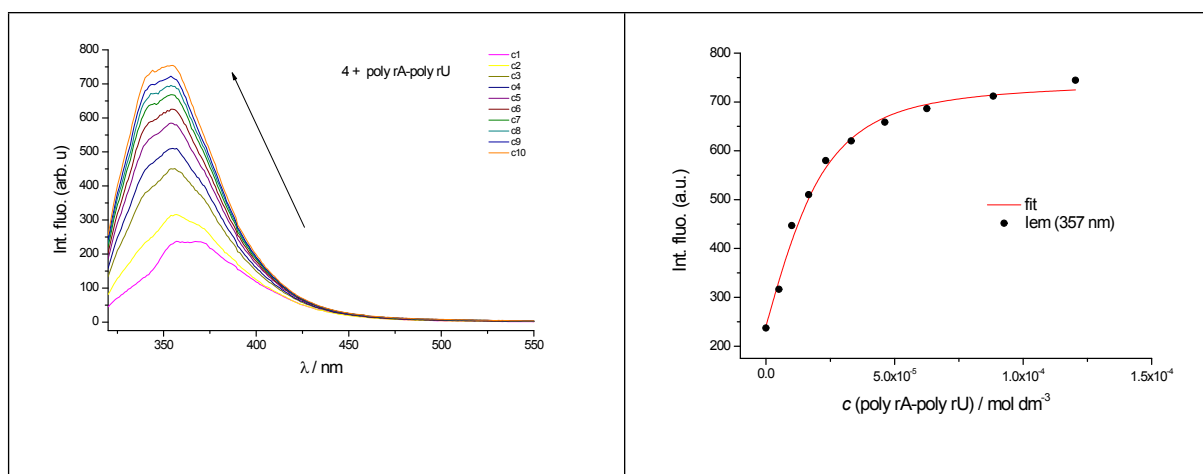


Figure S 24. Left: Fluorimetric titration of **4**, $\lambda_{\text{exc}} = 300 \text{ nm}$, $c = 2 \times 10^{-6} \text{ mol dm}^{-3}$ with poly rA–poly rU, Right: Experimental (●) and calculated (–) (by Scatchard eq., Table S2) fluorescence intensities of **4** at $\lambda_{\text{em}} = 357 \text{ nm}$ upon addition of ct DNA (pH = 5.0, Na cacodylate buffer, $I = 0.05 \text{ mol dm}^{-3}$).

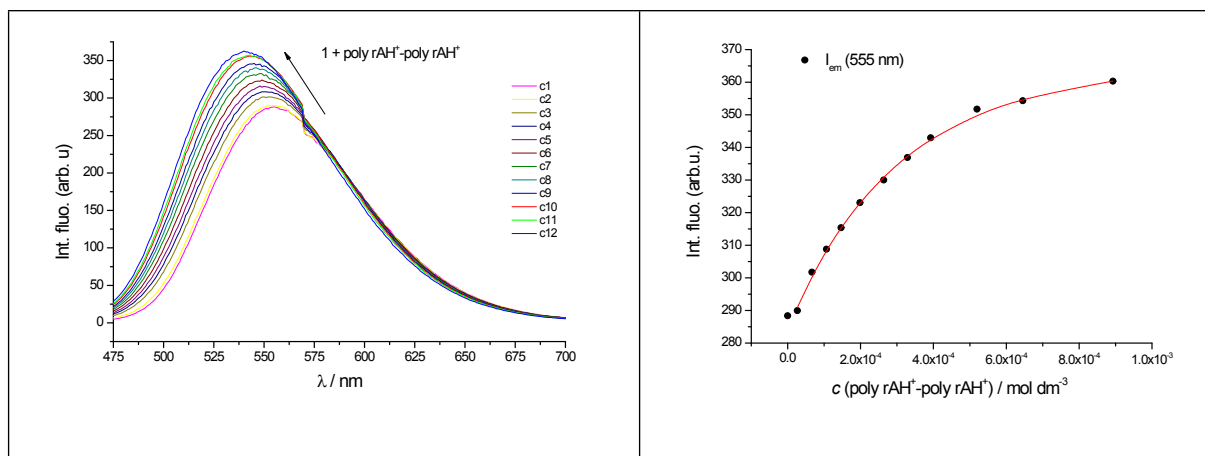


Figure S 25. Left: Fluorimetric titration of **1**, $\lambda_{\text{exc}} = 440 \text{ nm}$, $c = 2 \times 10^{-6} \text{ mol dm}^{-3}$ poly rAH⁺-poly rAH⁺, Right: Experimental (●) and calculated (—) (by Scatchard eq., Table S2) fluorescence intensities of **1** at $\lambda_{\text{em}} = 555 \text{ nm}$ upon addition of ct DNA (pH = 5.0, Na cacodylate buffer, $I = 0.05 \text{ mol dm}^{-3}$).

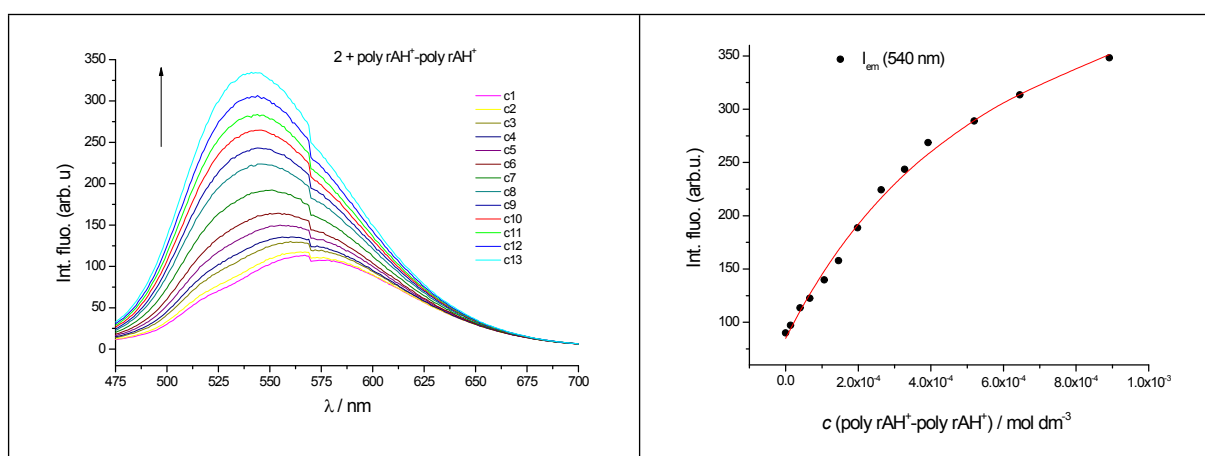


Figure S 26. Left: Fluorimetric titration of **2**, $\lambda_{\text{exc}} = 440 \text{ nm}$, $c = 2 \times 10^{-6} \text{ mol dm}^{-3}$ with poly rAH⁺-poly rAH⁺, Right: Experimental (●) and calculated (—) (by Scatchard eq., Table S2) fluorescence intensities of **2** at $\lambda_{\text{em}} = 540 \text{ nm}$ upon addition of ct DNA (pH = 5.0, Na cacodylate buffer, $I = 0.05 \text{ mol dm}^{-3}$).

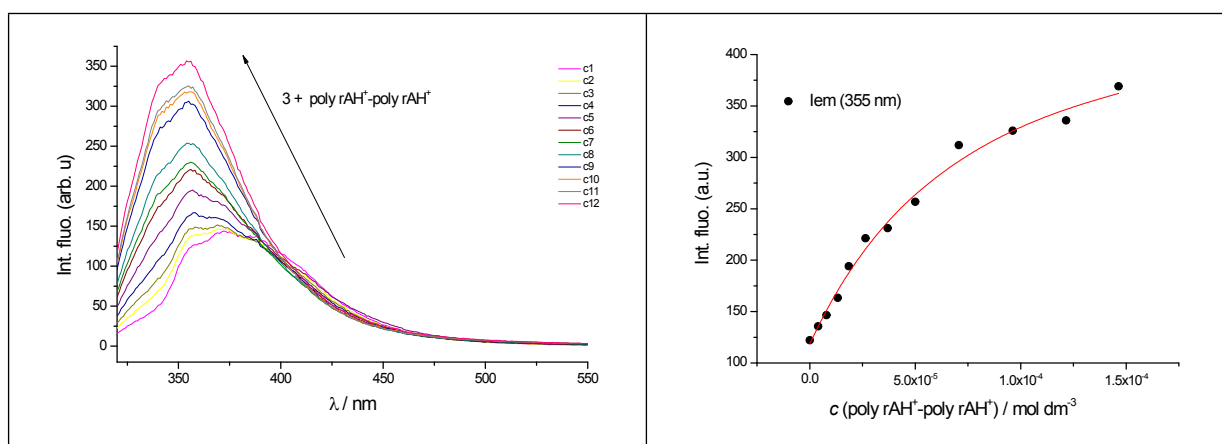


Figure S 27. Left: Fluorimetric titration of **3**, $\lambda_{\text{exc}} = 300 \text{ nm}$, $c = 2 \times 10^{-6} \text{ mol dm}^{-3}$ with poly rAH⁺-poly rAH⁺, Right: Experimental (●) and calculated (—) (by Scatchard eq., Table S2) fluorescence intensities of **3** at $\lambda_{\text{em}} = 355 \text{ nm}$ upon addition of ct DNA (pH = 5.0, Na cacodylate buffer, $I = 0.05 \text{ mol dm}^{-3}$).

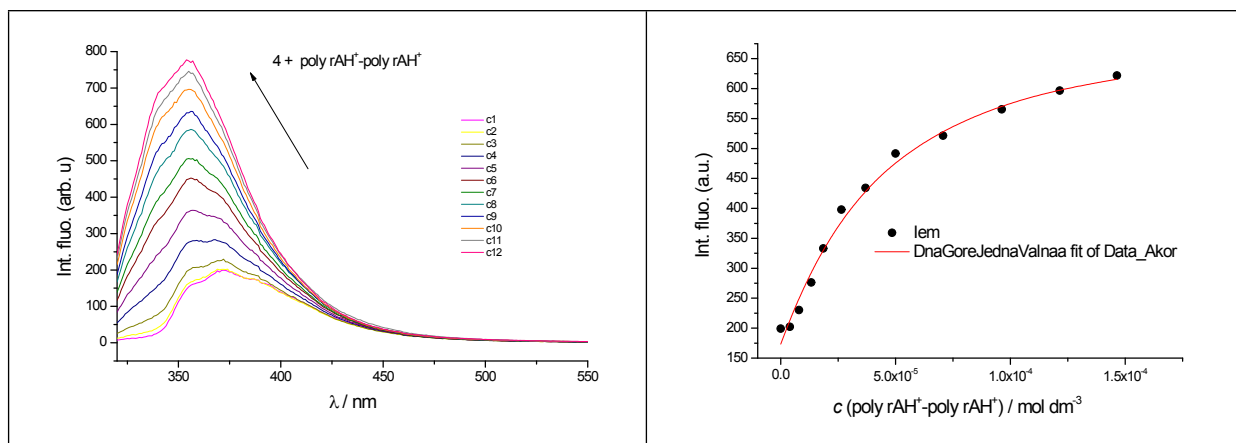


Figure S 28. Left: Fluorimetric titration of **4**, $\lambda_{\text{exc}} = 300 \text{ nm}$, $c = 2 \times 10^{-6} \text{ mol dm}^{-3}$ with poly rAH⁺-poly rAH⁺, Right: Experimental (●) and calculated (–) (by Scatchard eq., Table S2) fluorescence intensities of **4** at $\lambda_{\text{em}} = 357 \text{ nm}$ upon addition of ct DNA (pH = 5.0, Na cacodylate buffer, $I = 0.05 \text{ mol dm}^{-3}$).

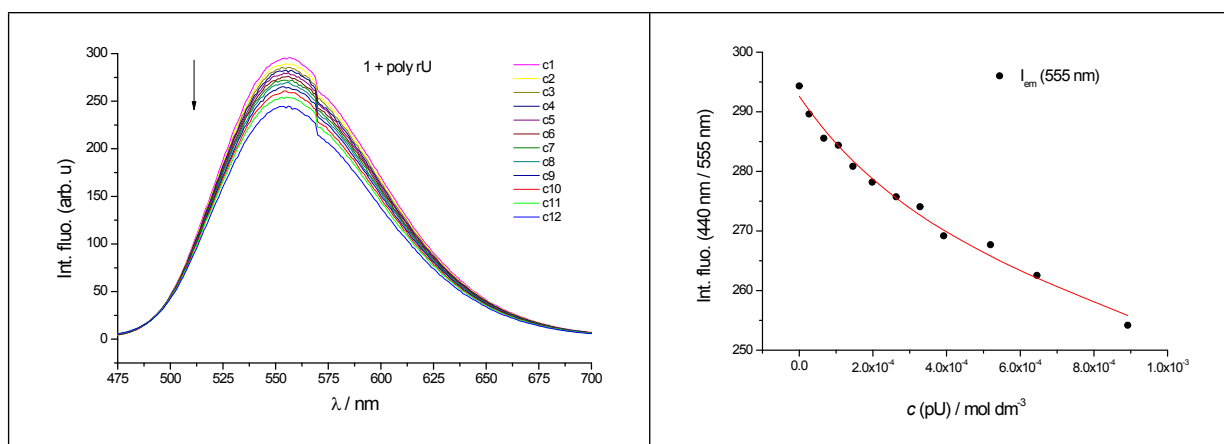


Figure S 29. Left: Fluorimetric titration of **1**, $\lambda_{\text{exc}} = 440 \text{ nm}$, $c = 2 \times 10^{-6} \text{ mol dm}^{-3}$ poly rU, Right: Experimental (●) and calculated (–) (by Scatchard eq., Table S2) fluorescence intensities of **1** at $\lambda_{\text{em}} = 555 \text{ nm}$ upon addition of ct DNA (pH = 5.0, Na cacodylate buffer, $I = 0.05 \text{ mol dm}^{-3}$).

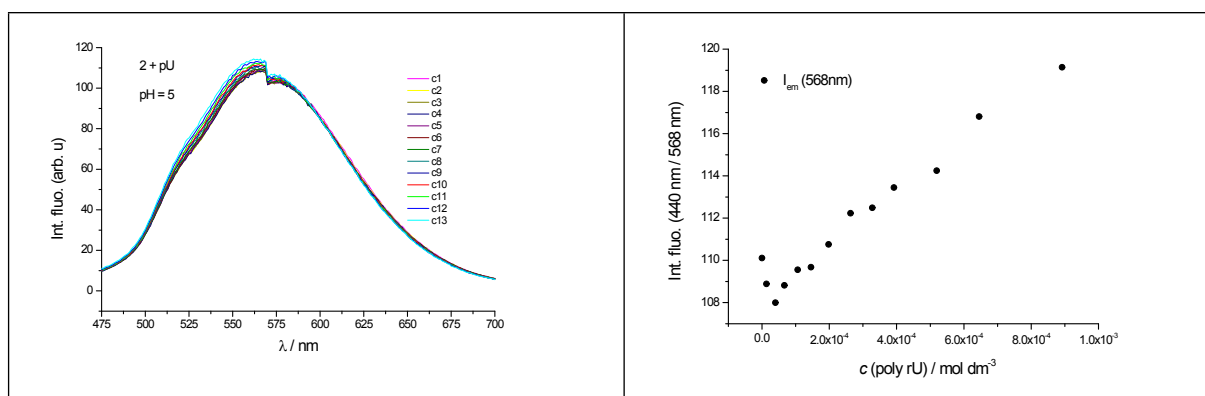


Figure S 30. Left: Fluorimetric titration of **2**, $\lambda_{\text{exc}} = 440 \text{ nm}$, $c = 2 \times 10^{-6} \text{ mol dm}^{-3}$ with poly rU, Right: Experimental (●) fluorescence intensities of **2** at $\lambda_{\text{em}} = 568 \text{ nm}$ upon addition of ct DNA (pH = 5.0, Na cacodylate buffer, $I = 0.05 \text{ mol dm}^{-3}$).

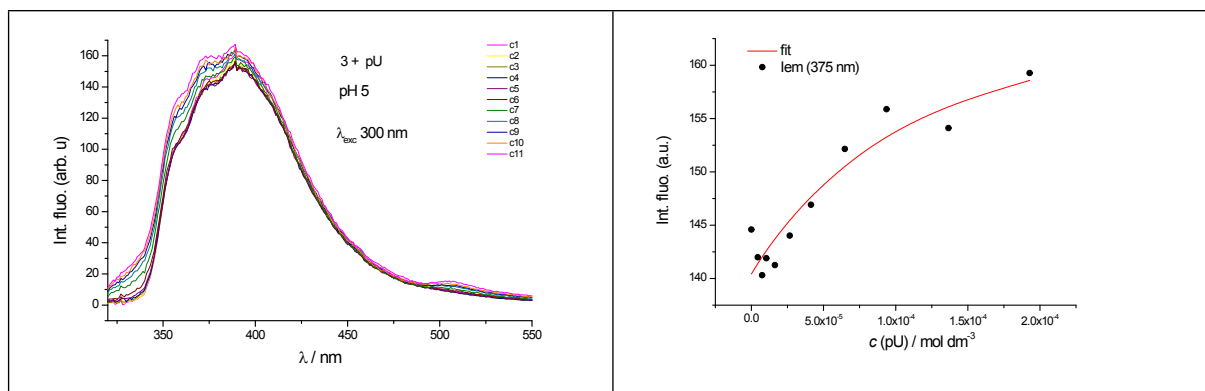


Figure S 31. Left: Fluorimetric titration of **3**, $\lambda_{\text{exc}} = 300 \text{ nm}$, $c = 2 \times 10^{-6} \text{ mol dm}^{-3}$ with poly rU, Right: Experimental (\bullet) and calculated ($-$) (by Scatchard eq., Table S2) fluorescence intensities of **3** at $\lambda_{\text{em}} = 375 \text{ nm}$ upon addition of ct DNA (pH = 5.0, Na cacodylate buffer, $I = 0.05 \text{ mol dm}^{-3}$).

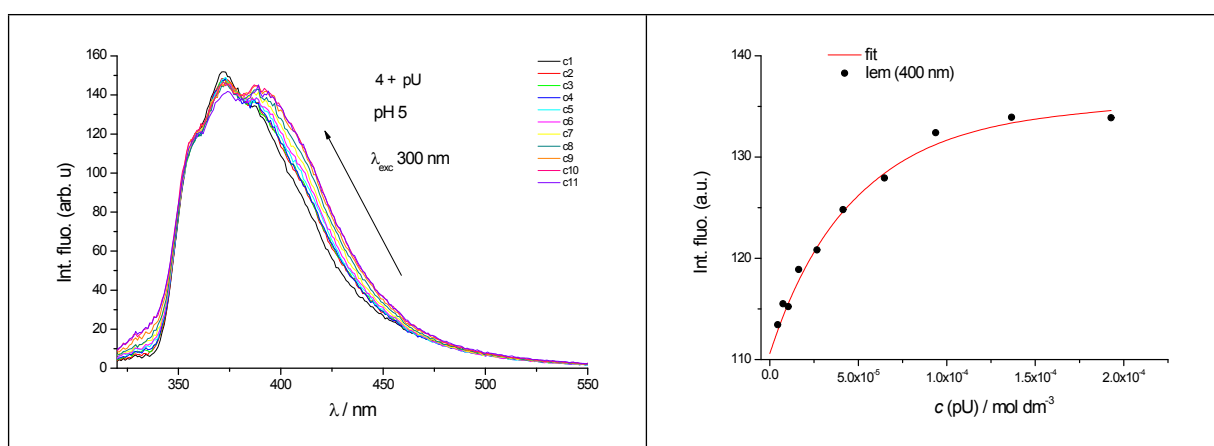


Figure S 32. Left: Fluorimetric titration of **4**, $\lambda_{\text{exc}} = 300 \text{ nm}$, $c = 2 \times 10^{-6} \text{ mol dm}^{-3}$ with poly rU, Right: Experimental (\bullet) and calculated ($-$) (by Scatchard eq., Table S2) fluorescence intensities of **4** at $\lambda_{\text{em}} = 400 \text{ nm}$ upon addition of ct DNA (pH = 5.0, Na cacodylate buffer, $I = 0.05 \text{ mol dm}^{-3}$).

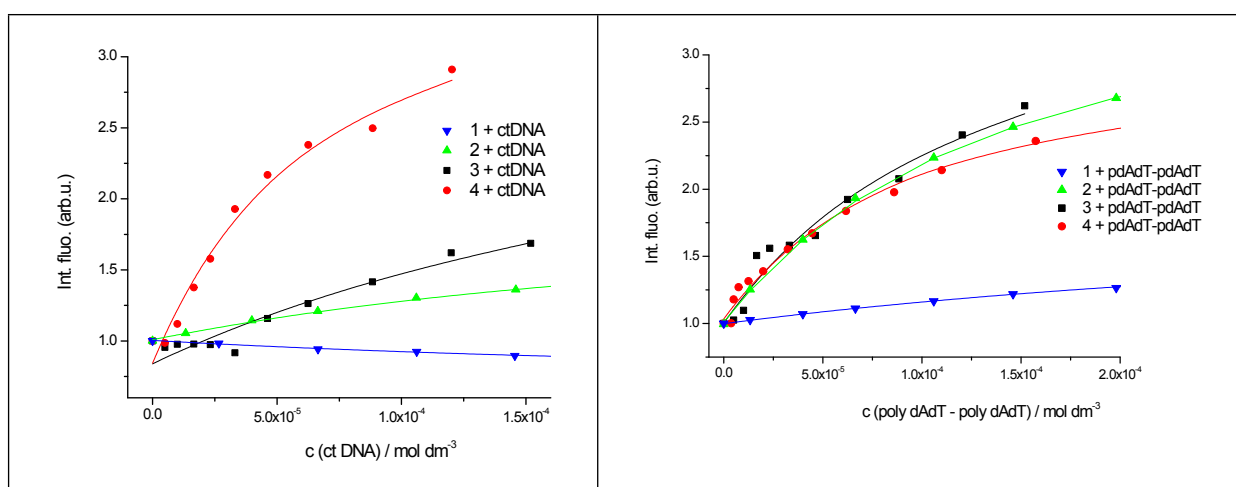


Figure S 33. Experimental (\blacksquare) and calculated ($-$) (by Scatchard eq., Table 2) fluorescence intensities of compounds **1-4** upon addition of ct DNA (left) and poly dAdT-poly dAdT (right); values were normalized for easier comparison. Na-cacodylate buffer, pH 5.0, $I = 0.05 \text{ M}$, $\lambda_{\text{exc}} = 440 \text{ nm}$ (**1, 2**) or $\lambda_{\text{exc}} = 300 \text{ nm}$ (**3, 4**).

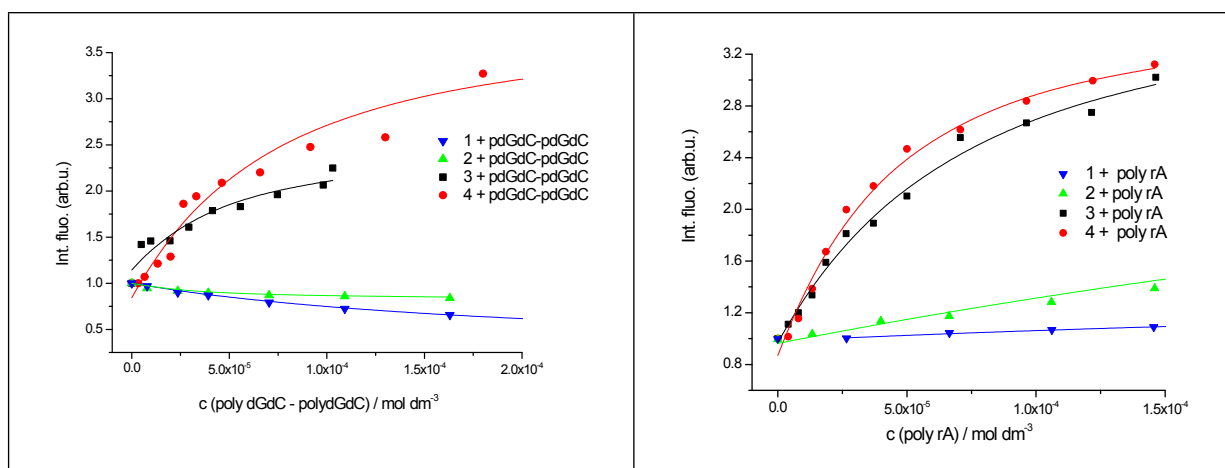


Figure S 34. Experimental (■) and calculated (–) (by Scatchard eq., Table 2) fluorescence intensities of compounds **1-4** upon addition of poly dGdC-poly dGdC (left) and poly rA^{H+}-poly rA^{H+} (right); values were normalized for easier comparison. Na-cacodylate buffer, pH 5.0, *I* = 0.05 M, λ_{exc} = 440 nm (**1, 2**) or λ_{exc} = 308 nm (**3, 4**).

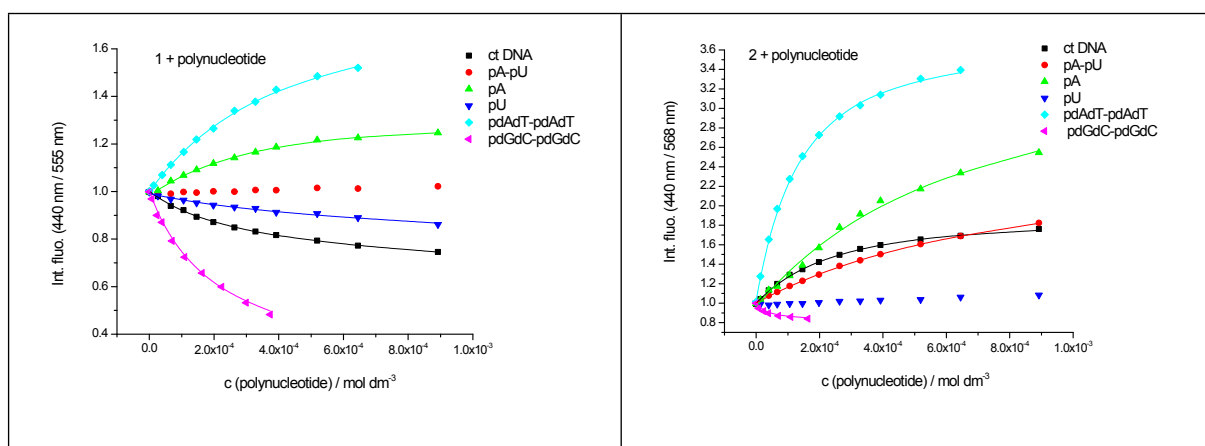


Figure S 35. Experimental (■) and calculated (–) (by Scatchard eq., Table 2) fluorescence intensities of compounds **1** (left) and **2** (right) upon addition of different polynucleotides; values were normalized for easier comparison. Na-cacodylate buffer, pH 5.0, *I* = 0.05 M, λ_{exc} = 440 nm.

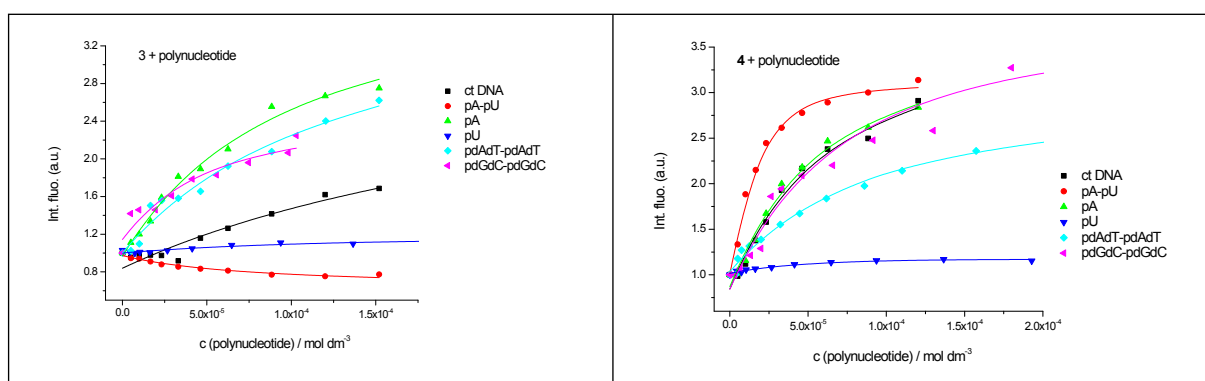


Figure S 36. Experimental (■) and calculated (–) (by Scatchard eq., Table ?) fluorescence intensities of compounds **3** (left) and **4** (right) upon addition of different polynucleotides; values were

normalized for easier comparison. Na-cacodylate buffer, pH 5.0, $l = 0.05$ M, $\lambda_{exc} = 440$ nm (**1**, **2**) or $\lambda_{exc} = 300$ nm (**3**, **4**).

3.3. Circular dichroism (CD) experiments

CD spectroscopy was chosen to monitor conformational changes of polynucleotide secondary structure induced by small molecule binding.

Unlike **1** and **2**, compounds **3**, **DS8** and **4** were built using chiral amino acid building blocks and consequently have intrinsic CD spectrum.

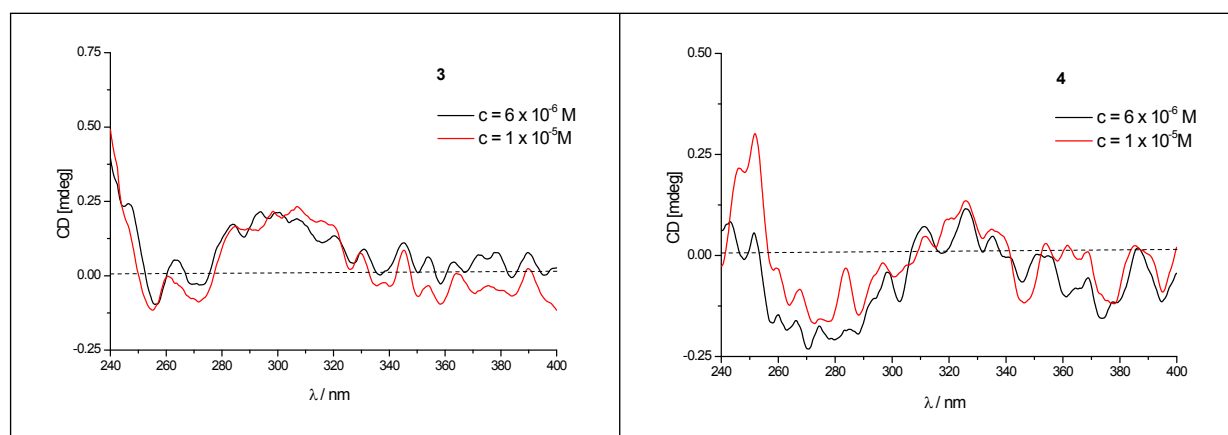


Figure S 37. CD spectra of **3** and **4** (Na-cacodylate buffer, pH 5.0, $l = 0.05$ M)

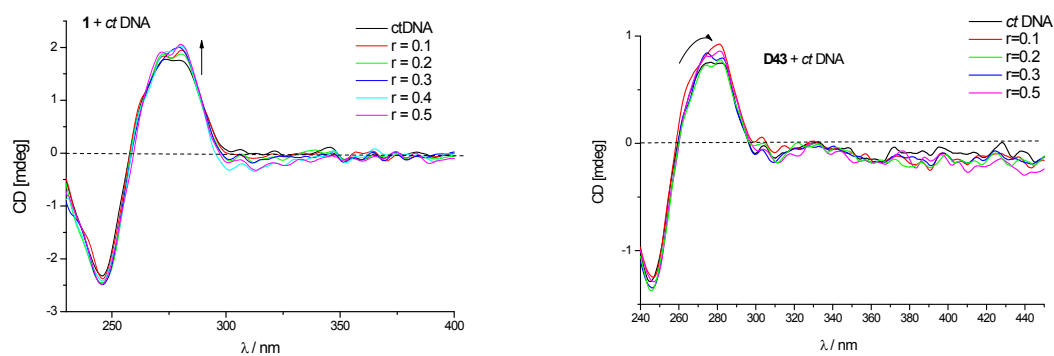


Figure S 38. Changes in the CD spectrum of *ct* DNA upon addition of **1** ($c(\text{DNA}) = 3 \times 10^{-5}$ mol dm^{-3}) (left) and **2** ($c(\text{DNA}) = 2 \times 10^{-5}$ mol dm^{-3}) (right) at different molar ratios $r = [\text{compound}] / [\text{polynucleotide}]$, pH = 5.0, sodium cacodylate buffer, $l = 0.05$ mol dm^{-3} .

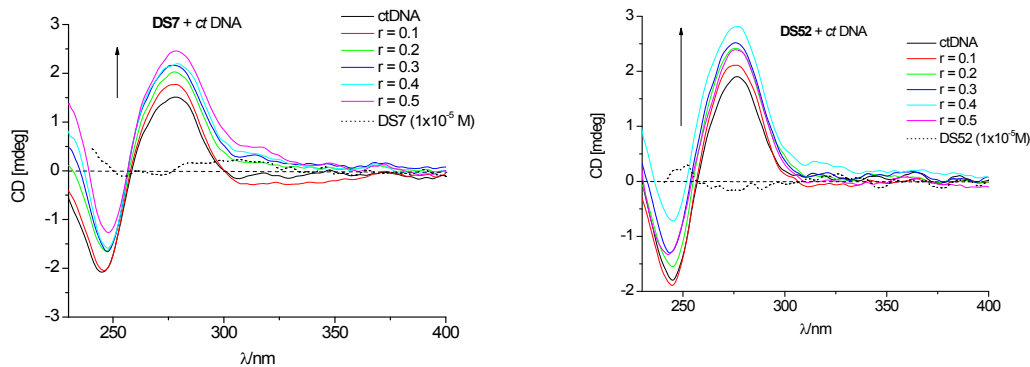


Figure S39. Changes in the CD spectrum of *ct* DNA ($c = 2 \times 10^{-5} \text{ mol dm}^{-3}$) upon addition of **3** (left) and **4** (right) at different molar ratios $r = [\text{compound}] / [\text{polynucleotide}]$, pH = 5.0, sodium cacodylate buffer, $I = 0.05 \text{ mol dm}^{-3}$.

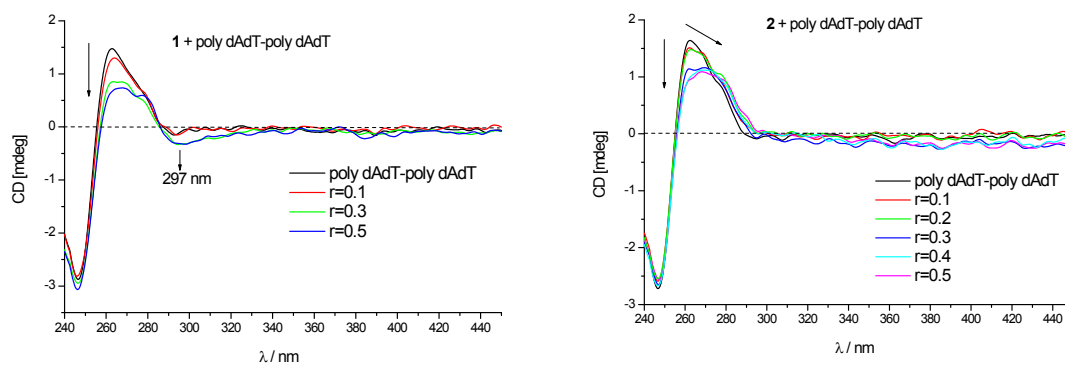


Figure S40. Changes in the CD spectrum of poly dAdT – poly dAdT ($c = 2 \times 10^{-5} \text{ mol dm}^{-3}$) upon addition of **1** (left) and **2** (right) at different molar ratios $r = [\text{compound}] / [\text{polynucleotide}]$, pH = 5.0, sodium cacodylate buffer, $I = 0.05 \text{ mol dm}^{-3}$.

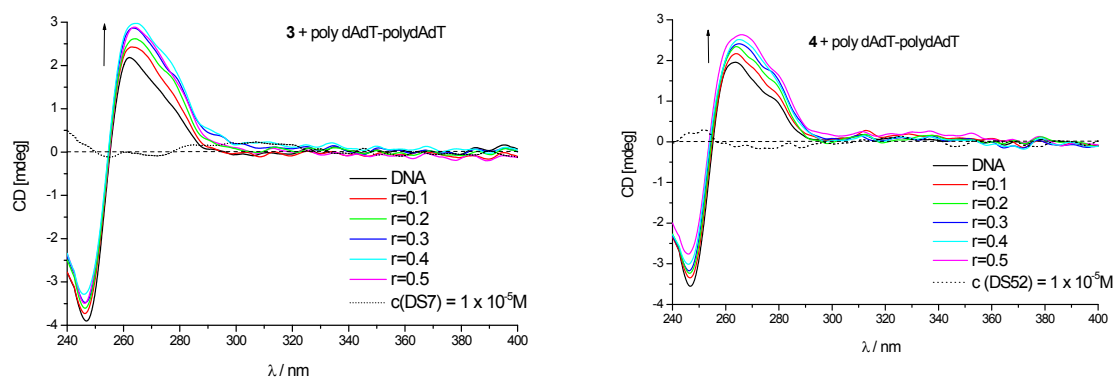


Figure S41. Changes in the CD spectrum of poly dAdT – poly dAdT ($c = 2 \times 10^{-5} \text{ mol dm}^{-3}$) upon addition of **3** (left) and **4** (right) at different molar ratios $r = [\text{compound}] / [\text{polynucleotide}]$, pH = 5.0, sodium cacodylate buffer, $I = 0.05 \text{ mol dm}^{-3}$.

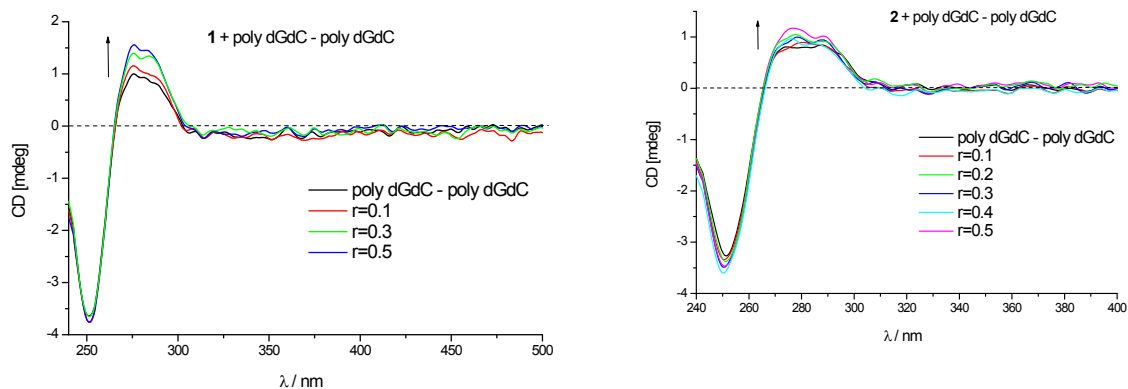


Figure S 42. Changes in the CD spectrum of poly dGdC – poly dGdC ($c = 2 \times 10^{-5} \text{ mol dm}^{-3}$) upon addition of **1** (left) and **2** (right) at different molar ratios $r = [\text{compound}] / [\text{polynucleotide}]$, pH = 5.0, sodium cacodylate buffer, $I = 0.05 \text{ mol dm}^{-3}$.

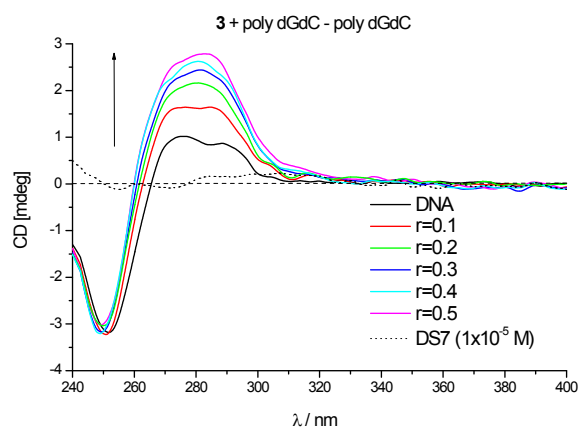


Figure S 43. Changes in the CD spectrum of poly dGdC – poly dGdC ($c = 2 \times 10^{-5} \text{ mol dm}^{-3}$) upon addition of **3** ($c(\text{DNA}) = 2 \times 10^{-5} \text{ mol dm}^{-3}$) (left) at different molar ratios $r = [\text{compound}] / [\text{polynucleotide}]$, pH = 5.0, sodium cacodylate buffer, $I = 0.05 \text{ mol dm}^{-3}$.

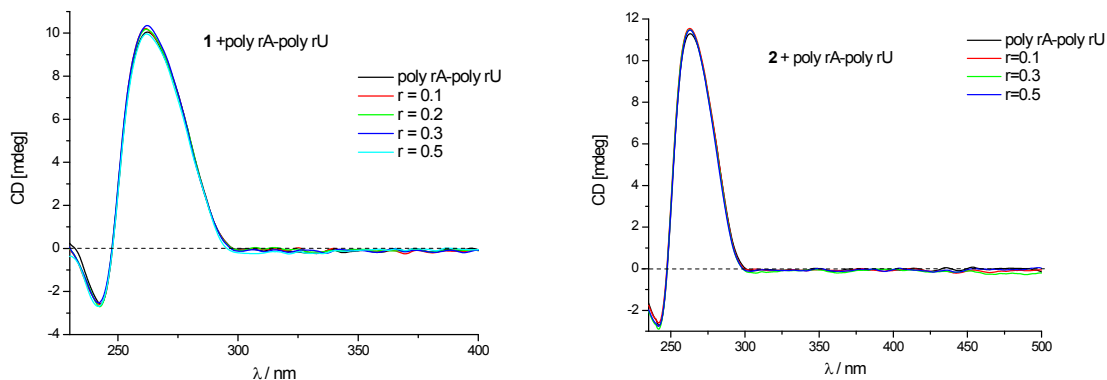


Figure S 44. Changes in the CD spectrum of poly rA-poly rU ($c = 3 \times 10^{-5} \text{ mol dm}^{-3}$) upon addition of **1** (left) and **2** (right) at different molar ratios $r = [\text{compound}] / [\text{polynucleotide}]$, pH = 5.0, sodium cacodylate buffer, $I = 0.05 \text{ mol dm}^{-3}$.

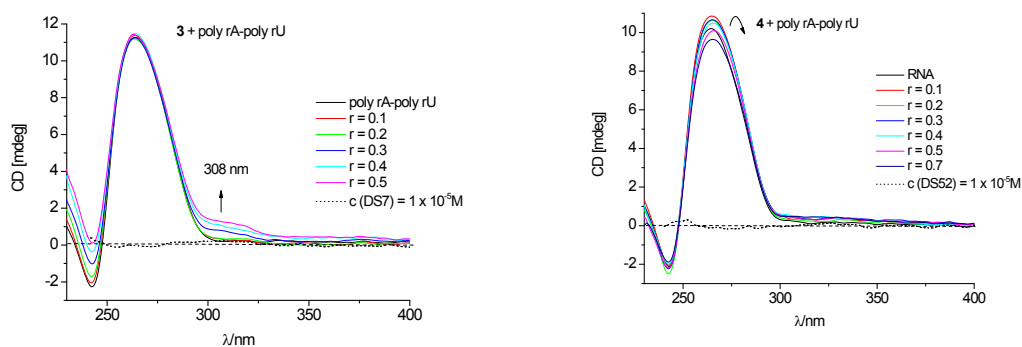


Figure S 45. Changes in the CD spectrum of poly rA-poly rU ($c = 3 \times 10^{-5} \text{ mol dm}^{-3}$) upon addition of **3** (left) and **4** (right) at different molar ratios $r = [\text{compound}] / [\text{polynucleotide}]$, pH = 5.0, sodium cacodylate buffer, $I = 0.05 \text{ mol dm}^{-3}$.

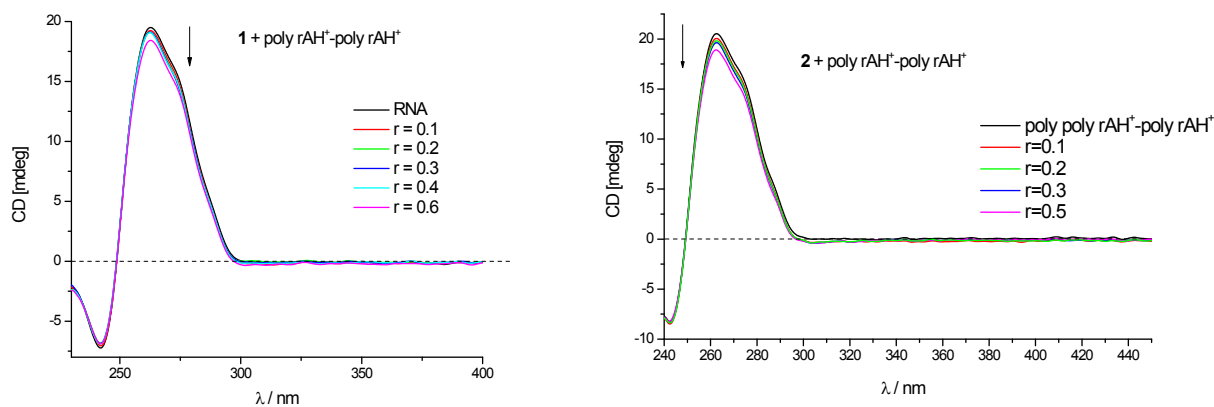


Figure S 46. Changes in the CD spectrum of poly rAH⁺-poly rAH⁺ ($c = 2 \times 10^{-5} \text{ mol dm}^{-3}$) upon addition of **1** (left) and **2** (right) at different molar ratios $r = [\text{compound}] / [\text{polynucleotide}]$, pH = 5.0, sodium cacodylate buffer, $I = 0.05 \text{ mol dm}^{-3}$.

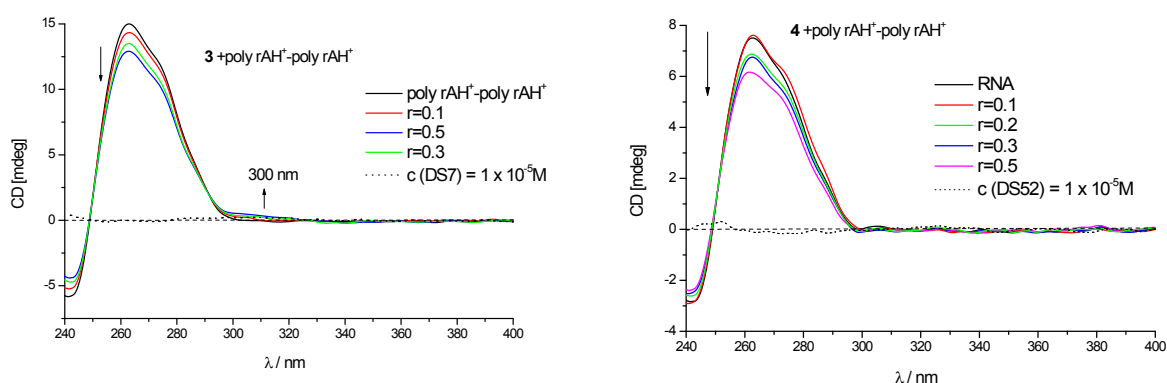


Figure S 47. Changes in the CD spectrum of poly rAH⁺-poly rAH⁺ ($c = 2 \times 10^{-5} \text{ mol dm}^{-3}$) upon addition of **3** (left) and **4** (right) at different molar ratios $r = [\text{compound}] / [\text{polynucleotide}]$, pH = 5.0, sodium cacodylate buffer, $I = 0.05 \text{ mol dm}^{-3}$.

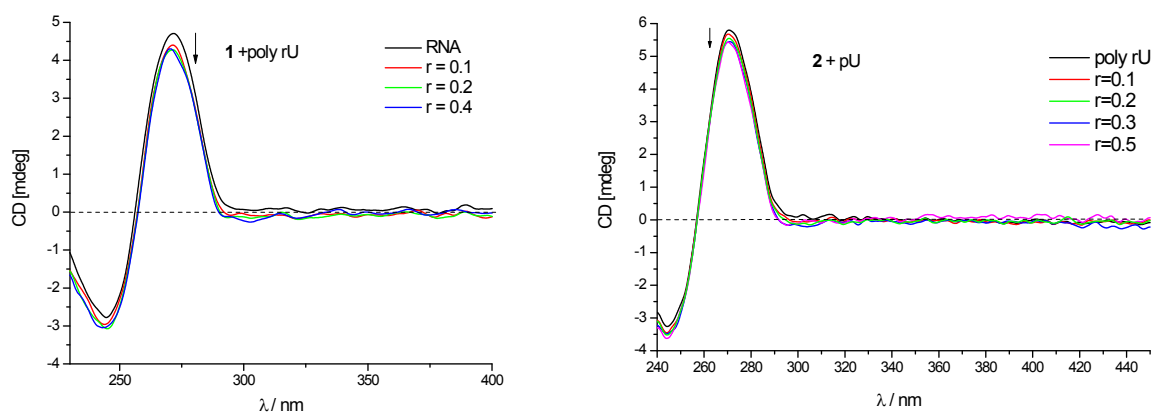


Figure S 48. Changes in the CD spectrum of poly rU ($c = 2 \times 10^{-5} \text{ mol dm}^{-3}$) upon addition of **1** (left) and **2** (right) at different molar ratios $r = [\text{compound}] / [\text{polynucleotide}]$, pH = 5.0, sodium cacodylate buffer, $I = 0.05 \text{ mol dm}^{-3}$.

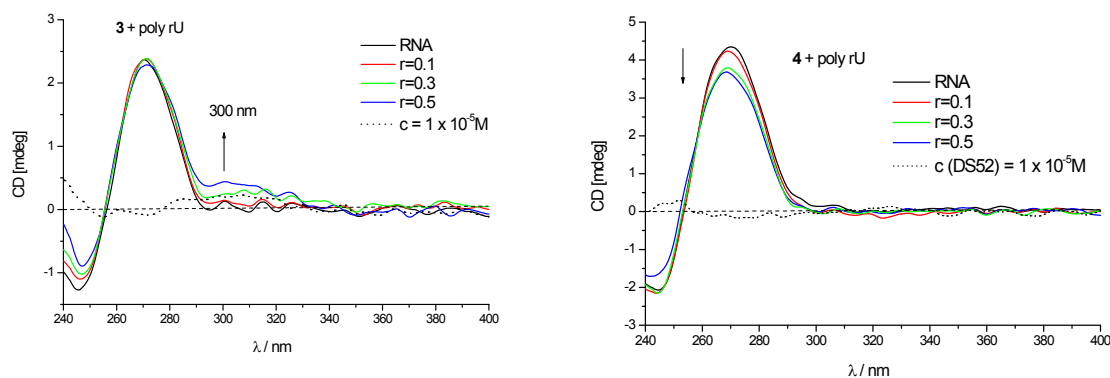


Figure S 49. Changes in the CD spectrum of poly rU ($c = 2 \times 10^{-5} \text{ mol dm}^{-3}$) upon addition of **3** (left) and **4** (right) at different molar ratios $r = [\text{compound}] / [\text{polynucleotide}]$, pH = 5.0, sodium cacodylate buffer, $I = 0.05 \text{ mol dm}^{-3}$.

4. Biological Activity

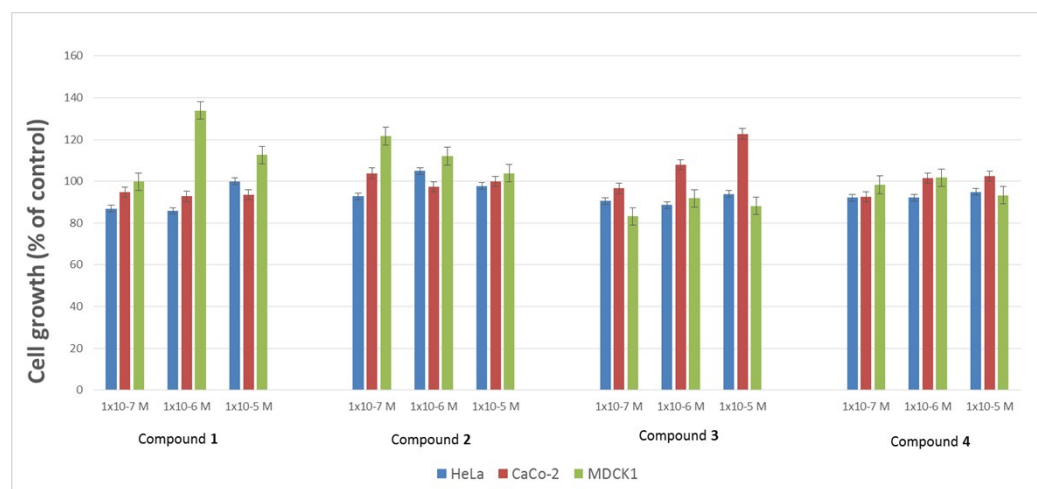


Figure S 50. Dose-response profiles for compounds **1-4** tested in vitro on a human tumour cell lines HeLa, CaCo2, and normal epithelial cells (MDCK1). Data represents mean values \pm standard deviation

(SD) of three independent experiments. Exponentially growing cells were treated during 72-hrs period. Cytotoxicity was analysed using MTT survival assay.

5. MM2 calculations

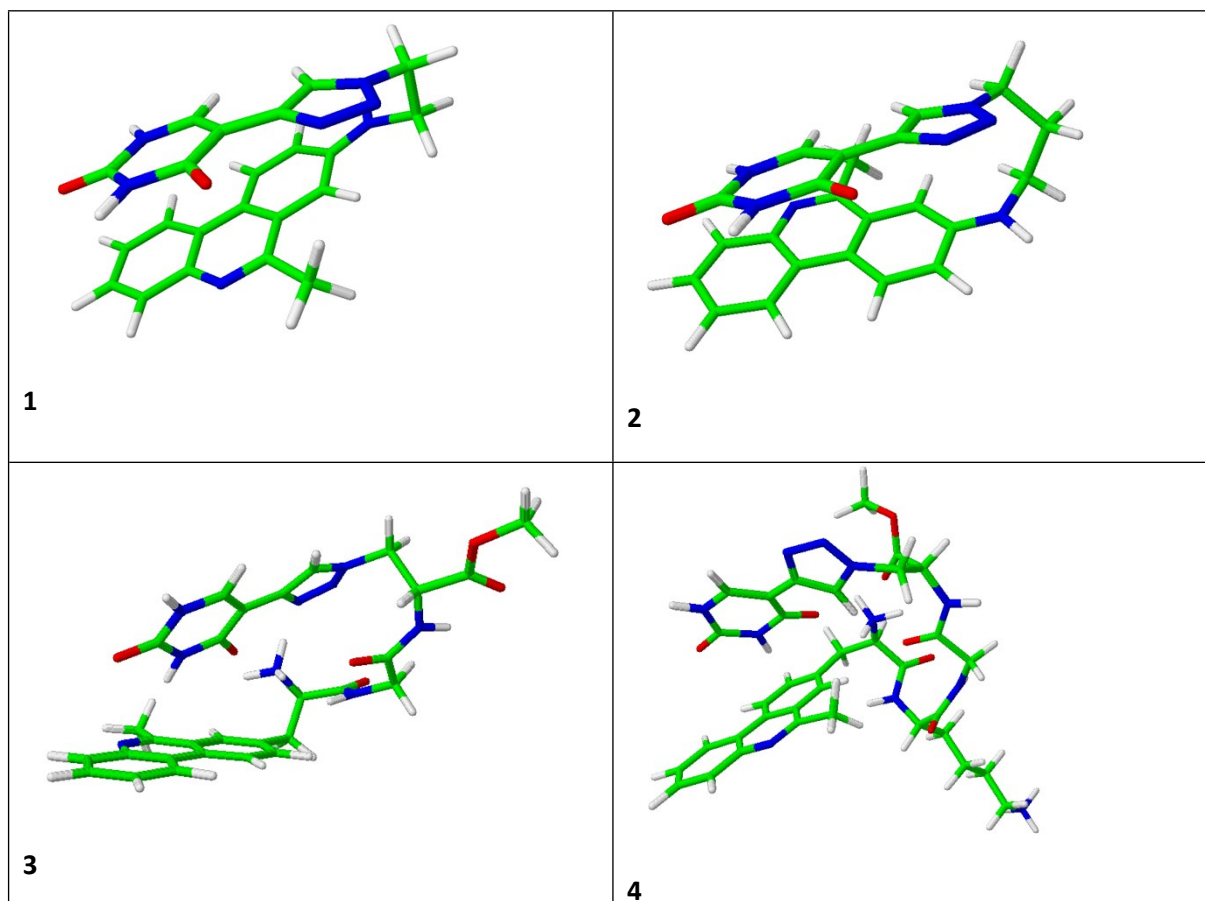


Figure S 51 **1-4** were submitted to MM2 calculations by a modified version of Allinger's MM2 force field, integrated into the ChemBio3D 11.0 programme, whereby obtained structures demonstrate the possible intramolecular aromatic stacking between phenanthridine and triazolyluracil.

1 L.-M. Tumir, I. Piantanida, P. Novak, M. Žinić, *J. Phys. Org. Chem.*, 2002, **15**, 599.

2 Dukši, Marko; Baretić, Domagoj; Čaplar, Vesna; Piantanida, Ivo. , *European journal of medicinal chemistry*. 2010, **6**, 2671-2676.

3 (a) M. Dukši, D. Baretić and I. Piantanida, *Acta Chim. Slov.*, 2012, **59**, 464–472. (b) M. Dukši, D. Baretić, V. Čaplar and I. Piantanida, *Eur. J. Med. Chem.*, 2010, **6**, 2671-2676.

4 (a) E. D. Goddard-Borger and R. V. Stick, *Org. Lett.*, 2007, **9**, 3797–3800. (b) Y. H. Lau and D. R. Spring, *Synlett*, 2011, **13**, 1917–1919.

5 J. B. Chaires, N. Dattagupta and D. M. Crothers, *Biochemistry* 1982, **21**, 3933.

6 T. V. Chalikian, J. Völker, G. E. Plum and K. J. Breslauer, *Proc. Natl. Acad. Sci. USA*, 1999, **96**, 7853-7858.

-
- 7 C. R. Cantor and P. R. Schimmel, *Biophysical Chemistry, Part. III*, W. H. Freeman and Co., San Francisco, 1980, 1145-1147.
- 8 C. Ciatto, M. L. D'Amico, G. Natile, F. Secco and M. Venturini, *Biophys. J.*, 1999, **77**, 2717-2724.
- 9 A. Das, K. Bhadra, B. Achari, P. Chakraborty and G. S. Kumar, *Biophys. Chem.*, 2011, **155**, 10-19.
- 10 Precipitation even to a small degree causes stray light effects, which generate irreproducibility of spectra, very often a intensity decrease with time, and pronounced differences between spectra of samples staying longer time and those taken instantly after mixing. A. Slama-Schwok and J.-M. Lehn, *Biochemistry*, 1990, **29**, 7895-7903. and ref. cited therein.
- 11 (a) J. D. McGhee and P. H. von Hippel, *J. Mol. Biol.*, 1974, **86**, 469-489. b) G. Scatchard, *Ann. N. Y. Acad. Sci.*, 1949, **51**, 660-672.
- 12 I. Crnolatac, I. Rogan, B. Majić, S. Tomić, T. Deligeorgiev, G. Horvat, D. Makuc, J. Plavec, G. Pescitelli, I. Piantanida, *Anal. Chim. Acta*, 2016, **940**, 128-135.
- 13 J. L. Mergny and L. Lacroix, *Oligonucleotides*, 2003, **13**, 515.
- 14 N. Horiuchi, K. Nagawa, Y. Sasaki, K. Minato, Y. Fujiwara, K. Nezu, Y. Ohe, and N. Sajo, *Cancer Chemother. Pharmacol.* 1988, **22**, 246–250.
- 15 G. Mickisch, S. Fajta, H. Bier, R. Tschada and P. Alken, *Urol. Res.*, 1991, **19**, 99–103.
- 16 W. Saenger, *Principles of Nucleic Acid Structure*, Springer-Verlag: New York, 1983; p. 226.